JPRS-UEQ-90-011
19 JULY 1990

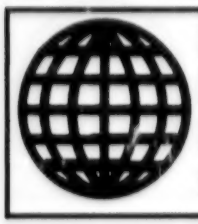

FOREIGN
BROADCAST
INFORMATION
SERVICE

JPRS Report

Science & Technology

USSR: Engineering & Equipment

Science & Technology
USSR: Engineering & Equipment

JPRS-UEQ-90-011 *19 July 1990*

CONTENTS

Nuclear Energy

High-Flux Bulk-Type Research Reactor With Partial Fuel Overloading
[Ya. D. Belyavskiy, D. I. Zhvirblya, et al.; IZVESTIYA AKADEMII NAUK BSSR SERIYA FIZIKO-ENERGETICHESKIKH NAUK, No 1, Jan-Mar 90] 1

Turbines, Engines, Propulsion Systems

Gimbal Drive With Tubes Made of Composite Materials
[S. N. Ivanov, N. P. Kocheskkov[1]; AVTOMOBILNAYA PROMYSHLENNOST, No 5, May 90] 5
Shock Absorber Based on Magnetic Fluid
[V. I. Boguslavskiy, M. I. Bronshteyn, et al.; AVTOMOBILNAYA PROMYSHLENNOST, No 5, May 90] 7
Connecting Rod Made of Composite Material
[A. S. Lukin, N. A. Starodubets, et al.; AVTOMOBILNAYA PROMYSHLENNOST, No 5, May 90] 8
Components Made of High-Strength Cast Iron
[V. A. Belov, A. V. Shlykova, et al.; AVTOMOBILNAYA PROMYSHLENNOST, No 5, May 90] 9
Effectiveness of Two-Loop Intake System in Internal Combustion Engine
[B. S. Stefanovskiy, A. T. Reppikh, et al.; AVTOMOBILNAYA PROMYSHLENNOST, No 5, May 90] .. 10
Antilocking Systems and Brake Drive Operation
[A. M. Galaktionov, V. V. Poluektov; AVTOMOBILNAYA PROMYSHLENNOST, No 5, May 90] 11
Architecture of Internal Combustion Engine Microprocessor Systems
[A. K. Giryavets, V. V. Muravlev, et al.; AVTOMOBILNAYA PROMYSHLENNOST, No 5, May 90] 12
Ergonomic Properties of Systems
[O. V. Mayboroda, V. V. Savelyev; AVTOMOBILNAYA PROMYSHLENNOST, No 5, May 90] 14

Industrial Technology, Planning, Productivity

Effect of Structural Condition of Coating on Performability of Cutting Tools
[V. V. Letunovskiy, A. V. Petruchenya, et al.; IZVESTIYA VYSSHIKH UCHEBNYKH ZAVEDENIY: MASHINOSTROYENIYE, No 3, Mar 90] 17
Investigation of Precision Characteristics of Feed Drives of Precision Lathe Modules
[B. M. Brzhozovskiy, M. V. Vinogradov, et al.; IZVESTIYA VYSSHIKH UCHEBNYKH ZAVEDENIY: MASHINOSTROYENIYE, No 3, Mar 90] 19
Classification of Automatic Assembly Equipment
[V. A. Serenko, V. G. Belomestnov; IZVESTIYA VYSSHIKH UCHEBNYKH ZAVEDENIY: MASHINOSTROYENIYE, No 3, Mar 90] 22
Assessing Design Decisions in Manufacturing Process CAD System by Simulation of Process of Manufacturing Components Under FMS Conditions
[V. A. Tsekhmeystruk, M. S. Ukolov; IZVESTIYA VYSSHIKH UCHEBNYKH ZAVEDENIY: MASHINOSTROYENIYE, No 3, Mar 90] 24
Conducting Service Life Tests on Flexible Bearings for Strain-Wave Gearing on Special Stands
[V. A. Finogenov, Ye. A. Sarayev; IZVESTIYA VYSSHIKH UCHEBNYKH ZAVEDENIY: MASHINOSTROYENIYE, No 3, Mar 90] 26

UDC 621.039.55

High-Flux Bulk-Type Research Reactor With Partial Fuel Overloading

907F0302A Minsk IZVESTIYA AKADEMII NAUK BSSR SERIYA FIZIKO-ENERGETICHESKIKH NAUK in Russian No 1, Jan-Mar 90 (manuscript received 4 May 89) pp 3-8

[Article by Ya. D. Belyavskiy, D. I. Zhvirblya, and B. A. Litvinenko, Nuclear Power Generation Institute, BSSR Academy of Sciences; first paragraph is verbatim IZVESTIYA AKADEMII NAUK BSSR SERIYA FIZIKO-ENERGETICHESKIKH NAUK English abstract]

[Text] A high-flux nuclear research reactor with spherical fuel elements has been considered. The possibility of using partial overloadings of fuel elements to improve the physical reactor characteristics has been shown.

The development of basic physics and material science research with neutron sources and an increased intensity and the production of isotopes has stimulated further progress in high-flux nuclear research reactors. Possible conceptions of such reactors have been developed in a number of recently published works.[1-3]

One work proposes a high-flux reactor (HFPBR) with a bulk core. In this type of reactor the core is formed by pouring small-diameter (about 500 μm) spherical fuel elements between surrounding, coaxially arranged, perforated cylinders. The core is cooled by pumping coolant (D_2O) in a radial direction. A developed heat transfer surface (about 100 cm^2/cm^3) makes it possible to reach a mean energy intensity of about 10 MW/l. The maximum thermal neutron flux density reaches a value of (1 to 2) x 10^{16} neutrons/(cm^2 x s) depending on the selection and arrangement of the moderator. A significant distinction of this reactor is the hydraulic loading and unloading of the spherical fuel elements, which is conducted daily or every 2 days. The short fuel cycle permits operation at a low fuel load (about 2 kg uranium 235) with a low content of fission products.

The operation of the reactor at a low (close-to-critical) load is the result of an attempt to increase the maximum thermal neutron flux in the trap. A high load leads to depression of the fuel flux both in the fuel layer and in the outer moderator. When beryllium or a heavy-water moderator is used or when they are used in a specified combination, it is possible, owing to a reduction in the load, to increase the maximum flux of thermal neutrons by a factor of 2 to 2.5.[3]

Partial fuel overloading, during which the amount of fissioning uranium nuclei located in the core may also be reduced significantly, thus resulting in a gain in the maximum magnitude of the thermal neutron flux, is possible within the framework of the proposed model of a high-flux reactor. In addition, a partial fuel overloading mode makes it possible to increase the mean depth of fuel burnup, which has a favorable effect on the cost of producing thermal neutrons. Some results of computational research on the effect of partial fuel overloadings of spherical fuel elements on the physical characteristics of a bulk-type high-flux reactor with water as the coolant and moderator and a beryllium reflector are presented below. Light water was selected as the coolant and moderator in an attempt to discover the possible advantages of partial fuel overloading in a bulk-type high-flux reactor with a cheaper and more technologically feasible medium than heavy water.

The filling of spherical fuel elements in the proposed reactor is located between two cylindrical coaxial grids that are permeable by the coolant. The coolant is pumped in a radial direction—from the center to the periphery. Between the neutron trap and filling there is a distribution channel, and between the filling and side reflector there is a coolant discharge channel. The channels have cross sections that are variable throughout their height and that are intended to convert the coolant's axial motion to a radial motion and to distribute the coolant in a manner corresponding to the energy liberation profile. The core is surrounded with end and side reflectors made of beryllium. The fuel composition of the spherical fuel elements and the core's construction materials are analogous to these adopted in the high-flux reactor described elsewhere.[4]

Table 1 presents the key characteristics of the high-flux reactor, and Figure 1 depicts the radial distribution of the thermal neutron flux for some possible loads of uranium 235 in this reactor. Unlike in a heavy-water reactor, no strong dependence of the maximum thermal neutron flux on the load of fissioning material is observed. However, an increase in the leakage of thermal neutrons directly from the fuel layer into the trap dose not, in the given case, exert a noticeable effect on the formation of the maximum thermal neutron flux owing to relatively high absorption in ordinary water.

Table 1. Principal Characteristics of the High-Flux Reactor

Parameter	Value
Fuel composition	U_3O_8 + Al
Fuel density, g/cm^3	3.0
Diameter of spherical fuel elements,mm	2.5
Core height, cm	46
Core diameter, cm	29
Diameter of "neutron trap," cm	13
Thickness of pouring spherical fuel elements, cm	8
Volume fraction of fuel elements in fuel layer	0.6
Coolant	H_2O
Area of heat removal surface, m^2	35
Density of energy liberation in fuel layer, MW/l	4
Thermal capacity of reactor, MW	100

Table 1. Principal Characteristics of the High-Flux Reactor (Continued)

Parameter	Value
Coolant temperature:	
at inlet to core, °C	60
at outlet from core, °C	200
Coolant pressure, MPa	6.0
Hydraulic resistance of core, MPa	0.03

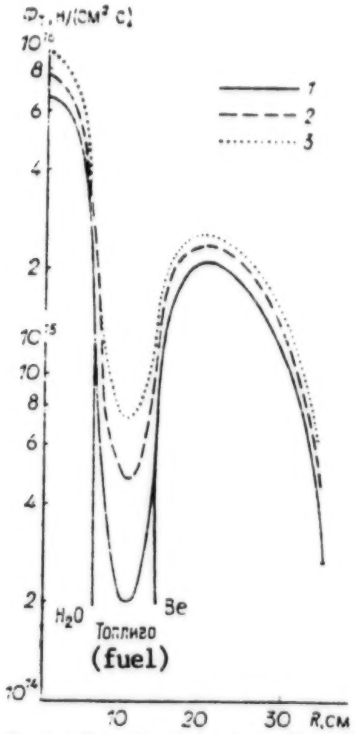

Figure 1. Radial Distribution of the Flux Density of Thermal Neutrons as a Function of the Load of Uranium 235: 1. 13.1 kg, K_{ef} = 1.16; 2. 6.5 kg, K_{ef} = 1.085; and 3. 4.5 kg, K_{ef} = 1.03.

The physical design of the reactor is implemented in a diffusion approximation with representation of the neutron spectrum in terms of 10 energy groups, one of which is thermal.[5] The KRATER program, which implements this method, is intended for engineering calculations of nuclear reactors (including a calculation of burnup). The program has its own library of nuclear data for 59 isotopes. A geometric model of the core may be represented in two-dimensions cylindrical and in three-dimensional (x, y, z) or hexagonal geometries. The program has been tested by designing uranium-water heterogeneous critical assemblies in a wide range of values of the ratio of the hydrogen concentration to the uranium 235 concentration.

The high-flux reactor under examination is, however, rather complex to design, and the possibility of using a diffusion approximation requires additional substantiation. This is due mainly to the presence of a water cavity in the center of the core, a neutron spectrum that is variable throughout the thickness of the fuel layer, and significant thermal neutron flux gradients close to the trap and reflector. For this purpose, a high-flux isotope reactor (HFIR) was designed in accordance with the KRATER program. The computation results are in satisfactory agreement with data from a previous work.[4] The value of K_{ef} in the beginning of the refueling cycle is underestimated by more than 1.0 percent. The nonperturbed thermal neutron flux density in the center of the trap of the HFIR equals 5.5 x 10^{15} neutrons/(cm^2 x s), whereas the calculated value is 4.7 x 10^{15} neutrons/(cm^2 x s). The error in estimating the volumetric coefficient of the unevenness of energy liberation does not exceed 5 percent. In addition, verification calculations of the high-flux reactor were conducted on the basis of the MMK-22 program.[6] It has been established that the difference in design parameters obtained on the basis of the KRATER program and the MMK-22 program meets the precision of engineering calculations. In regions where energy liberation flare-ups may occur, the calculated values of the thermal neutron fluxes differ by 10 to 12 percent, which can be explained primarily by the errors in the diffusion approximation.

A subprogram called CYCLE operating in a unified system with the KRATER program was created to calculate a steady-state mode of partial fuel overloadings. The method of formal renumeration of the reactor's zones is implemented in the subprogram, which makes it possible to automate the calculation of partial fuel overloadings and to determine the required characteristics of a steady-state mode of partial fuel overloadings: the period of partial overloadings, enrichment of the replenished fuel, reactivity time change, distribution of energy release, fluxes, etc.

Table 2 presents the key design parameters of the high-flux reactor with different versions of fuel overloading. The first version of fuel overloading stipulates one-time overloading of the entire core at the end of a refueling cycle. Versions 2 through 4 are variations of a steady-state mode of partial fuel overloadings for three schemes of the fuel's motion—axial motion of the fuel elements along three annular zones with a specified radial velocity profile (1.5:1:1.5) and one-time passage through the core and radial motion also along three annular zones in accordance with the "in-out" and "out-in" principles. Selection of the scheme's of the spherical fuel elements' motion reflects the specifics of a bulk-type high-flux reactor and is due largely to the presence of flare-ups of energy liberation in regions adjacent to the trap and reflector. It is proposed that, to implement such schemes of motion, the filling of spherical fuel elements be divided by two coaxial cylinders that can be penetrated by the coolant and that each of the three overloading zones be provided with its own system for loading and unloading fuel elements.

Table 2. Key Design Parameters of the High-Flux Reactor With Different Versions of Refueling

Parameter	Versions of Refueling			
	1	2	3	4
Reactor's thermal capacity, MW	100	100	100	100
Energy intensity of fuel layer, MW/l	4.0	4.0	4.0	4.0
Thickness of refueling zones, cm:				
zone I	8.0	2.0	3.4	3.4
zone II	—	4.0	2.5	2.5
zone III	—	2.0	2.1	2.1
Period between refuelings, days	20	5	10	10
Time fuel elements are in core, days	20	36	30	30
Time to refuel core, hr	2.0	0.5	2.0	2.0
Amount uranium 235 loaded during refueling, kg	12.9	1.81	4.3	4.3
Burnup of discharged fuel (fima), percent:				
maximum	45.0	48.2	34.0	32.0
average	15.0	27	22.5	22.5
Average (throughout core) burnup of fuel at end of burnup cycle (before refueling) (fima), percent	15.0	15.2	15.1	15.0
Excess reactivity after refueling, percent	14.0	1.2	1.9	1.7
Reactivity margin at end of burnup cycle (before refueling), percent	1.1	0.9	1.0	1.0
Maximum thermal neutron density, neutrons/(cm^2 x s):				
in neutron trap	6.9×10^{15}	8.2×10^{15}	8.10×10^{15}	8.0×10^{15}
in beryllium reflector	2.1×10^{15}	2.5×10^{15}	2.4×10^{15}	2.4×10^{15}

It follows from Table 2 that a significant (by a factor of 1.5 to 1.8) increase in the depth of fuel burnup is achieved in a steady-state mode of partial fuel overloadings when compared with that in the version with one-time overloading. The consumption of fuel elements in the process of the high-flux reactor's operation is reduced in the same ratio, which noticeably improves the economic operating indicators.

In the case where the fuel moves in accordance with "in-out" and "out-in" schemes, the reactor's characteristics in a steady-state mode of partial fuel overloadings are practically identical. This apparent inconsistency is due to certain distinctive features of the high-flux reactor under examination. First, the dimensions of the reactor's core are rather small—the length of the neutrons' migration is comparable with the thickness of the fuel layer. Second, highly enriched fuel (90 percent) is used. Third, the side reflector is made of beryllium and hardly absorbs thermal neutrons, whereas ordinary water is located in the trap. As a result, it turns out that the value of the neutrons close to the trap and reflector is approximately identical.

Axial fuel motion is organized throughout three annular zones; however, the thicknesses of the zones are changed somewhat and selected such that the characteristic portion of the energy liberation profile (flare-ups or the sloping segment) comes entirely into the respective zone. The speed and time for which the spherical fuel elements are in the core are determined from the condition that the limit allowable fuel burnup not be exceeded. When the fuel elements' motion is organized in a similar manner, it is possible to achieve a deeper burnup of the discharged fuel. This is because, first, at the end of the burnup cycle the average burnup throughout the core for all four versions of overloading the fuel elements coincides with sufficient precision, amounting to 15.0-15.2 percent. This means that, at that moment, approximately one and the same quantity of uranium 235 nuclei remain in the core, thereby creating a reactivity margin of 0.9 to 1.1 percent depending on the distribution throughout the core. Second, in the case of the second version of overloading, a higher ratio of replenished and discharged, but not spent atoms of uranium 235, is achieved.

Figure 2 presents the change in the reactivity margin over time as a function of the version of fuel overloading. It follows from Figure 2 that for all three modes of partial fuel overloading, the value of the maximum excess reactivity is significantly (approximately threefold) less than that in a mode without partial overloadings. This fact is of no small importance and ultimately makes it possible to reduce the amount of movable elements in the reactor control and protection system, thereby increasing nuclear safety.

The change in reactivity in the initial moment after the partial fuel overloading is defined as a transient xenon process. If the partial overloading is conducted in a

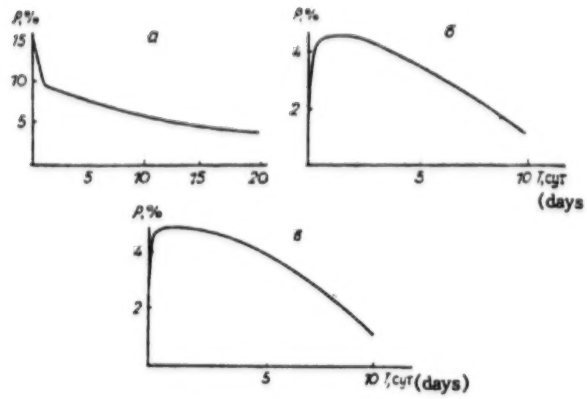

Figure 2. Change in the Reactor's Reactivity Margin Throughout Its Refueling Cycle: a, in the Case of One-Time Fuel Overloading (version 1); b and c, in a Steady-State Mode of Partial Fuel Overloadings During Axial Movement of the Fuel (version 2) and Displacement of the Fuel in Accordance With the "In-Out" Principle (version 3).

reactor that has been shut down, there is an accumulation (and decay) of xenon 135 in the spent fuel during the overloadings. Depending on the duration of this period, the concentration of xenon 135 may reach a value that is several times in excess of the steady-state value. This is especially critical for high-flux reactors since the steady poisoning in them when highly enriched fuel is used approaches the limit amount of 5 percent. In view of this, rather strict constraints have been imposed on the partial overloading time. As the calculations show, in the case of radial motion of the fuel (versions 3 and 4) the overloading time must not exceed 2 hours, and in the case of axial motion (version 2) it must not exceed 0.5 hours. The reality of similar times is confirmed experimentally on a hydraulic stand. However, these experiments were preliminary in nature, and further comprehensive research is needed to derive well-founded recommendations.

When partial fuel overloadings are used, a smaller amount of uranium 235 is located in the core than in the case of one-time overloading, which increases the level of the neutron flux and, consequently, the magnitude of the leakage of neutrons into the trap and reflector. The maximum thermal neutron flux both in the case of axial motion of the fuel (version 2) and radial motion (versions 3 and 4) increases by approximately 20 percent. This result conforms to the estimate presented in Figure 2 and is explained by the increase in the leakage of moderated neutrons into the trap. It should, however, be noted that we are speaking of a qualitative comparison of the results. The resultant increase in the maximum thermal neutron flux is at the precision level of the calculation of this quantity and amounts to 15-20 percent. Nevertheless, since different, albeit rather close states of one and the same reactor (that have been calculated in accordance with one and the same program) are being compared, a qualitative comparison of the results is possible. When heavy water or beryllium is used as the trap material, the role of the leakage of thermal neutrons in the formation of the thermal neutron flux in the trap is significant. This is due to the weak absorption in these materials. According to others'[3] estimates, in this case it is possible to increase the maximum thermal neutron flux by a factor of 2 to 2.5.

The results of calculations of the proposed modes of partial fuel overloadings confirm the possibility of improving the technical and economic characteristics of high-flux reactors when compared with the case of the conventional version of one-time overloading. However, using light water as a moderator in a high-flux reactor does not make it possible to significantly increase the maximum thermal neutron flux on account of a reduction in the load of fissioning material. When heavy water or beryllium is used as the moderator in this type of reactor, it is not only possible to achieve better technical and economic indicators but also to achieve a significant increase in the maximum thermal neutron flux.

Bibliography

1. Lace, J. A., et al., TRANS. AMER. NUCL. SOC., Vol 52, 1986, pp 64-646.

2. Worley, B. A., et al., TRANS. AMER. NUCL. SOC., Vol 49, 1985, p 422.

3. Powell, J. R., Takahashi, H., and Horn, F. L., NUCL. INSTR. AND METHODS IN PHYS. RESEARCH A 249, 1986, pp 66-76.

4. Dzhan, A., Sartu, A. L., Blok, T. Ye., et al., "Oakridge Isotope Reactor With High-Density Neutron Flux," in "Dokl. na III Mezhdunarodnoy konferentsii po mirnomu ispolzovaniyu atomnoy energii" [Reports at Third International Conference on Peaceful Use of Atomic Energy], Geneva, 1964, 27 pages.

5. Savushkin, I. A., Rubin, I. Ye., Dneprovskaya, N. M., et al., VESTSI AN BSSR. SER. FIZ.-ENERG. NAVUK, No 3, 1987, pp 5-10.

6. Frank-Kamenetskiy, A. D., "Programma mnogogruppovykh raschetov reaktorov i yacheyek metodom Monte-Karlo" [Program for Multigroup Design of Reactors and Cells by Using Monte Carlo Method], Moscow, 1978, 18 pages (Preprint/IAE imeni I. V. Kurchatov, No 2148).

COPYRIGHT: Vydavetstva "Navuka i tekhnika" Vestsi AN BSSR, seryya fizika-energetychnykh navuk, 1990

UDC 629.113-585.862.233.1-036.5.419.8

Gimbal Drive With Tubes Made of Composite Materials

907F0314G Moscow AVTOMOBILNAYA PROMYSHLENNOST in Russian No 5, May 90 pp 15-17

[Article by S. N. Ivanov, doctor of technical sciences, and N. P. Kocheskkov, Central Automobile and Automotive Scientific Research Institute, Scientific Technical Center of the Volga Automotive Plant imeni 50th Anniversary of the USSR]

[Text] In the development of modern technology, including in auto manufacturing, there has been a steady trend toward replacing conventional materials by polymer composites. Their area of application is continually expanding and now includes components of the running gear, propulsion unit, transmission, and particularly the gimbal drive—especially the cardan shaft. The point is that the geometry and design of the latter permit more successful realization of the advantages of fiber-reinforced polymers, their advantages over steels and even over aluminum alloys from the standpoint of the vehicle's technical and economic indicators. For example, the high strength and rigidity characteristics of composite materials on a polymer base in conjunction with their low density make it possible to reduce the rotating masses of transmissions and, as a result, fuel consumption and the vibroacoustic load of the vehicle's car. A low propagation rate of main cracks, high fatigue characteristics and damping properties, and a significant corrosion resistance are very important positive qualities of polymer composites. In addition, the total cost of producing polymer composites is less than that required to produce steel, for example, since the manufacture of components and structures in a composite version is a low-waste process.

However, making the advantages of polymer composites a reality requires reinforcing them correctly—by selecting reinforcing elements (carbon, glass, and aramid fibers are used most often) and binders and by selecting the block diagram used to arrange these elements in layers.

The most rational diagram, which considers the features of the loading of a cardan shaft in a transmission and the requirements regarding structural symmetry of the composite, is shown in Figure 1.

The following is characteristic for such schematics. If carbon fibers are used as the reinforcing element, they are placed at an 18-35° angle to the tube's rotation axis. If glass fibers are used, the angle in the outer layer should amount to 90°, and that in the inner layer should equal 45°. The smaller angles of the carbon fibers' orientation should be used for high-speed passenger car gimbal drives experiencing low loads, whereas the larger angles should be used in trucks with greater torques and lower speeds.

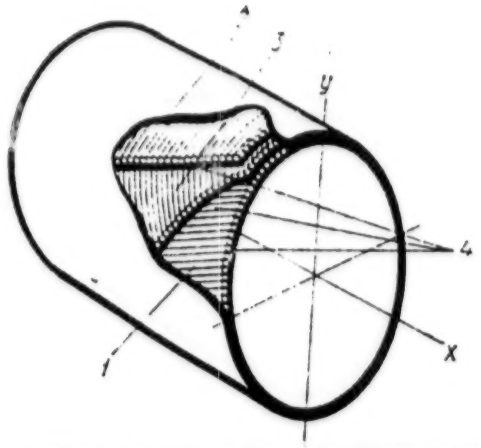

Figure 1. Block Diagram of the Arrangement of Fibers in a Composite Tube for a Gimbal Drive

Key: 1. glass fibers located at a 30-45° angle to the rotation axis; 2. glass fibers located at a 90° angle to the rotation axis; 3. carbon or aramid fibers located at an 18-30° angle to the rotation axis; 4. epoxy binders

The reasons for this strict approach to selecting the fibers' slopes are well known: the elasticity modulus of polymer composite is not constant along its different directions and depends precisely on the angle of the fibers' orientation with respect to the X and Y axes (see Figure 1). For the composite KMU-3 with unidirected fibers, for example, the elasticity modulus E_x with a fiber slope of 0° amounts to 17×10^{-4} MPa, whereas at 20° it is already 10.5×10^{-4} MPa, and at 50° it is only 2.2×10^{-4} MPa. The modulus relative to the Y axis changes in a virtually mirror image manner: at the same angles it amounts to 0.4×10^{-4} MPa, 1×10^{-4} MPa, and 17×10^{-4} MPa.

Like shafts made of conventional materials, cardan shafts with composite tubes are designed for the critical rotation frequency, strength, and resistance to buckling (with an allowance for the necessary safety factors, of course).

One example of the use of shafts made of composite is the VAZ vehicle with a classic transmission configuration. This is a two-shaft gimbal drive with a flexible coupling, movable splined joint, two cardan hinges, and an intermediate support in the form of a ball bearing that is mounted in a rubber-and-metal case connected to the body. Vibrations are transmitted through the intermediate bearing to the body. Reducing them effectively requires additional engineering decisions related to the design of the components on the bearing itself and the other elements of the gimbal drive and, in some cases, the entire transmission. It is not always possible to implement these designs in ordinary transmissions with an allowance for the requirements of configuring the vehicle and mass production technology. As far as a

composite gimbal drive is concerned, the problem is much simpler to solve—by eliminating the intermediate bearing from their design.

Furthermore, the designs of gimbal drives with steel pipes generally have a much greater mass and inertial moment than in the case of composite gimbal drive analogues since the density of steel is five times greater than the density of polymer composite. For example, a series-produced two-shaft gimbal drive for VAZ-2104, VAZ-2105, and VAZ-2107 has a mass of 10.8 kg and an inertial moment of 0.011 kg x m^2. The mass of the prototype single-shaft gimbal drives with no intermediate bearings and with composite tubes that have been developed for these transmissions and manufactured ranges from 4.8 to 6.3 kg, and their inertial moments range from 0.0035 to 0.0069 kg x m^2. The one that is the heaviest and that has the greatest inertial moment is a gear in which one composite tube has been replaced by two shafts, with the flexible coupling, movable splined joint, and two cardan hinges being kept (Figure 2b). A second design (Figure 2c) with a composite tube, flexible coupling, universal ball hinge, and equal angular velocity (providing angular and axial movements in the gear) had a mass of 5.1 kg and an inertial moment of 0.0065 kg x m^2. The distinction of the operation of this gear in a transmission is its high evenness of rotation (owing to the absence of cardan hinges with unequal angular velocities) and, consequently, its low levels of torsional and flexural vibrations.

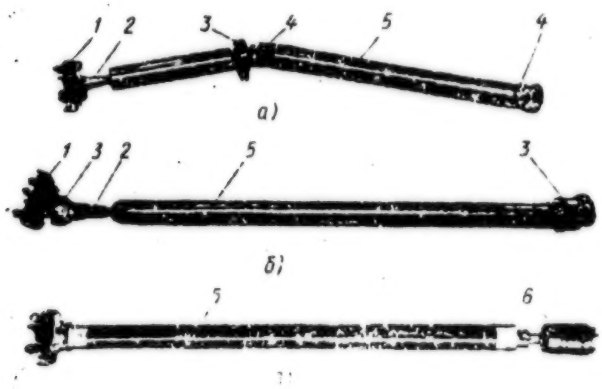

Figure 2. Structure of Gimbal Drives—Series-Produced (a) and With Tubes Made of Composites (b and c)

Key: 1. flexible coupling; 2. movable splined joint; 3. cardan hinges; 4. shaft; 5. tubes made of composite; 6. hinge

But the gimbal drive with a composite tube, two cardan hinges with uneven angular velocities, and a movable splined joint had the least mass and inertial moment. In addition, owing to the absence of a flexible rubber coupling, it has a torsional rigidity that was three times higher. (Its torsional rigidity coefficient amounts to 67 N x m/degree, whereas that of other shafts, including series-produced ones, is 22 N x m/degree). The reduction in mass and inertial moment and increase in torsional rigidity are factors that permit these shafts to operate under extremely difficult conditions, for example, in the transmissions of VAZ recreation vehicles. But the first two of the factors mentioned also improve their mass production consumer qualities, specifically their dynamics and fuel economy. Comparative calculations of the acceleration time of a VAZ-2105 based on individual gears and their fuel consumption for versions with series-produced and composite gimbal drives (the mass and inertial moment of which represent the average values of the three designs developed [see above]) showed the following: the time required for acceleration from the lowest (first) gear was reduced by 0.15 percent, that required for acceleration from the highest (fifth) gear was reduced by 0.09 percent, and the specific fuel consumption was reduced an average of 10 g/100 km. It must nevertheless be said that the effect of the mass and inertial moment of a composite gimbal drive on the dynamic and fuel economy qualities of a vehicle are less significant than is the effect of the inertial moments and masses of such rotating components as the engine's flywheel and the vehicle's drive wheels. The following is also understood: the absolute values of the masses and inertial moments here are different; therefore, changes in them are not expressed identically.

The prototypes of the composite gimbal drives developed have undergone road tests with an average course of 15,000 km. During their course, it was established that new cardan shafts significantly reduce vibrations and noises in the transmission. Specifically, special comparative tests proved that in a VAZ-2105 vehicle with a load that is 50 percent of the rated load, the intensity of the vibrations in the crankcase of the rear axle's reducing gear was reduced in a wide frequency range of its vibrations in a vertical direction, with the greatest reduction in vibration speeds being observed in the range of frequencies in excess of 1000 Hz. As the results of measuring the internal noise at standardized points (GOST 19358-85) in the front and rear seats during accelerations and even speeds of the vehicle confirm, this helps reduce noise in the car. Thus, during acceleration in fourth gear in the speed range from 60 to 120 km/h, the internal noise in the front seat was an average of 1 dBA lower and an average of 0.5 dBA lower in the rear seat. When the vehicle was moving at a constant speed (100 km/h) in fifth gear, these values amounted to 2.5 and 3.5 dBA, respectively.

Also evaluated during the experiments were the effect of a composite gear on the intensity of the load on the transmission by "peak" torques occurring during getaway and when changing gears. The results are presented in Table 1.

Table 1.

Phase of Vehicle's Motion	"Peak" Torque of Series-Produced Gear			"Peak" Torque of Composite Gear		
	Amount of Distribution	Median Variation, N x m	Mean Square Deviation, N x m	Amount of Distribution	Median Variation, N x m	Mean Square Deviation, N x m
Getaway in 1st gear	128	404	39	128	421	37
Gear changes:						
From 1st to 2nd	128	255	28	127	302	40
From 2nd to 1st	128	190	25	128	201	27
From 2nd to 3rd	128	220	26	120	206	40
From 3rd to 2nd	128	306	35	122	299	38

The peak dynamic loads in the transmission of a VAZ-2105 vehicle correspond to the normal distribution law. During changes from first to second gear the median torque of a transmission with a composite gimbal drive is 1.18 times less than that of a series-produced transmission (with a mean square deviation of the peak torques that is less by a factor of 1.4, i.e., the indicator of the spread of the experiments' results). The highest "peak" loads in a transmission occur during getaway, after which the loads start to moderate during changes from first to second and from second to first gear as well as from third to second and from second to third gear, which is characteristic for transmissions with both the series-produced and composite gimbal drive. The median "peak" torque during changes from first to second gear in a transmission with a composite gimbal drive is 16 percent less that in the case of a series-produced gear. In all remaining phases of motion the difference in the median values of the "peak" torques may be considered insignificant (it does not exceed 6 percent). The spread of the values of the "peak" torques is less in the transmission with the composite gimbal drive. A significant (not less than by a factor of 1.4) reduction in the mean square deviation is observed during changes from first to second gear and from third to second gear.

Thus, in the transmission of a VAZ-2105 with a composite gimbal drive, the maximum values of the "peak" torques with one and the same low probability will appear lower than in a transmission with a series-produced gimbal drive design. This makes it possible to assert that using a composite gear always reduces the intensity of the load on the transmission by "peak" torques.

The calculations and experiments performed show that composite gimbal drives significantly improve the vibroacoustic qualities of vehicles, reduce the dynamic loads of transmissions, and help improve the dynamic and fuel economy indicators of passenger cars. Especially interesting in this sense are gears with tubes made of polymer composites in all-wheel-drive vehicles with multiple-shaft designs and significant vibroacoustic activity of their transmissions.

Footnote

1. V. P. Petunin, L. V. Badun, and A. A. Vanovskiy took part in this work.

COPYRIGHT: Izdatelstvo "Mashinostroyeniye", "Avtomobilnaya promyshlennost",1990

UDC 629.113.012.813

Shock Absorber Based on Magnetic Fluid

907F0314H Moscow AVTOMOBILNAYA PROMYSHLENNOST in Russian No 5, May 90 p 17

[Article by V. I. Boguslavskiy, M. I. Bronshteyn, and V. V. Vodolazhchenko[1], Kharkov Automotive and Highway Institute, AvtoKrAZ Production Association, KF [not further identified] Kharkov Polytechnic Institute imeni V. I. Lenin]

[Text] Magnetic fluid in the shock absorber makes it possible to change the parameters of a vibration isolation system depending on the vibration frequency. This type of shock absorber is a ferromagnetic cylinder separated by a ferromagnetic piston and rod into two cavities. The gap between the piston and cylinder is filled with magnetic fluid that acts as a device controlling the passage of air between the cavities. This is accomplished as follows. An electrical winding is located around the rod. When voltage is fed to it, the fluid loses its capability of flowing out of the gap and thus seals the gap. Because the magnetic force holding the fluid in the gaps depends on the amount of voltage in the winding, changing it can specify the force at which the passage of air between the cavities begins, i.e., the beginning of the shock absorber's operation.

Figure 1 shows the actual design of such a shock absorber that was developed jointly by the Kharkov Automotive and Highway Institute and the Kremenchug Automotive Plant imeni the 50th Anniversary of the Soviet Ukraine. It is a ferromagnetic cylinder (1) separated by a ferromagnetic piston (2) and ferromagnetic rod (3) so as to form air-filled cavities (4 and 5). A ferromagnetic cap (6) holds a winding (7) inside the cylinder (1). Caps (8 and 9) are provided to seal the cavities (4 and 5). They are made of nonmagnetic material. The inner surface of the cavities is coated with a wetting magnetic fluid (10). When

voltage is fed to the winding (7), a magnetic flux is formed that is shown by arrows. The magnetic fluid (10) is drawn into the region of maximum magnetic induction, fills the annular gap between the piston and cylinder, and thereby forms a magnetic fluid seal. The cavities (4 and 5) are thus separated from one another.

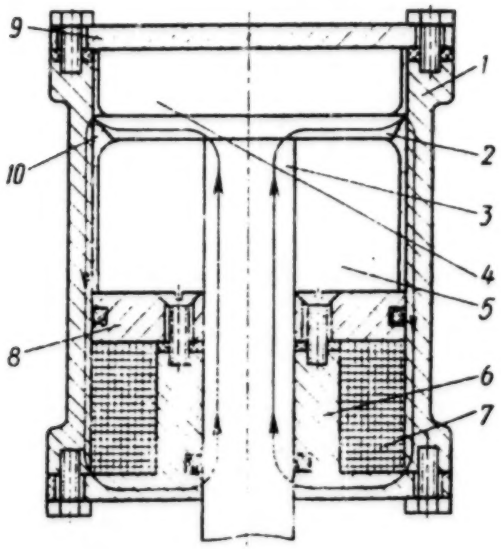

Figure 1

The piston moves inside the cylinder (1) when the vibration-isolated object, which is connected with the rod (3), vibrates. As the piston moves, for example, to the side of cavity (4), excess pressure is created in it, and the pressure in cavity (4) drops until the differential reaches the threshold for magnetic sealing of the level. From that moment, air begins to move through the magnetic fluid, and the pressure differential between the cavities remains constant.

Having reached the specified position corresponding to the given force on the rod, the piston begins to move to the opposite side. The pressure differential on the seal drops to zero, after which it changes sign and increases to the limit amount for magnetic fluid sealing of the level. Air is passed in the reverse direction, and the pressure differential between the cavities is again kept constant, but naturally with the opposite sign.

The shock absorber's design parameters are as follows: inner cylinder diameter, 60 mm; run of the piston, 100 mm. The rated voltage, current, and power of the winding amount to 12 V, 0.5 A, and 6 W, respectively; the shock absorber has a mass of 2.5 kg; the magnetic fluid amounts to 40 cm^3; and it has a magnetization of 120 kA/m.

The method of "semiactive" damping is used for the vibration isolation system. Its essence is as follows: the shock absorber is activated when it results in a reduction in the object's speed (the driver's seat in a KrAZ-260 vehicle) relative to the ground and does not operate otherwise. This is accomplished by sensors—two acceleration sensors mounted on the object being isolated from vibrations and the vibration stand's platform. The sensors' signals are integrated, and the relative speed of the object and the sign of the product of the object's speed times the relative speed are determined. The latter is the signal to switch the shock absorber on or off.

Comparative analysis of the amplitude-frequency characteristics of a seat taken for three cases (the series-produced version, without a series-produced or experimental shock absorber, and with the experimental shock absorber) shows that the control circuit based on the "semiactive" damping method with the experimental shock absorber makes it possible to reduce the transmission factor, which equals the ratio of the amplitude of the seat to the amplitude of the vibration stand's platform, in the resonance range to 1.25 versus 1.5 for a series-produced shock absorber. In the high-frequency range, the characteristics of the experimental circuit virtually coincide (from the standpoint of form) with the characteristics taken without a shock absorber; however, the transmission factor is cut to half that of the shock absorber in the series-produced seat for a KrAZ-260 vehicle.

Footnote

1. Ye. Ya. Kotlyar, I. N. Rumishevich, V. V. Tobolin (candidate of technical sciences), and I. V.Shevchenko took part in this work.

COPYRIGHT: Izdatelstvo "Mashinostroyeniye", "Avtomobilnaya promyshlennost",1990

UDC 621.43.232.1-036.5.419.8

Connecting Rod Made of Composite Material

907F0314F Moscow AVTOMOBILNAYA PROMYSHLENNOST in Russian No 5, May 90 p 15

[Article by A. S. Lukin, N. A. Starodubets, and Yu. Ye. Tyablikov, Moscow Auto Mechanics Institute]

[Text] Components manufactured from fiber composite materials have enjoyed increasing use in internal combustion engines in the past few years. True, it has been proved that such components reliably counteract mechanical loads only in the case where the filler's fibers coincide with the direction of the main tensile stresses. In view of this, there has been increasing interest in the problem of manufacturing internal combustion engine connecting rods from composite materials.

They consist of upper and lower heads (rings) that are generally metal, a rod (that may be made either metal or composite material), and a belt encompassing the connecting rod (made of unidirected composite material, i.e., carbon fiber) that receives a significant part of the tensile load acting on the connecting rod. The dimensions and shape of the belt depend on the design of the

lower head (detachable or nondetachable) and are calculated for static and dynamic strength with an allowance for the fact that the inelastic properties of composite materials worsen over time.

The main element of the connecting rod is the rod. It experiences loads with different magnitudes and directions. Its stressed state must therefore be investigated before it is manufactured.

Such research was conducted on a connecting rod consisting of metal rings that were glued together, a rod made of composite material, and a belt that was made of unidirected composite material and that encompassed the connecting rod. Its results confirm that, during compression, the greatest stress occurs at the points where the ring comes into contact with the center of the core and decreases quickly in the direction of its salient angles. In the center part of the rod the compressive stress along the cross section is practically constant. In addition, because of the difference in the elasticity moduli of the steel rings and the composite rod, an inhomogeneous stressed state that decreases as the rings' stiffness increases occurs at the places where they meet.

During extension of the rod, the nature of the stressed state in the zone where it makes contact with the rings changes fundamentally. The stress is not maximum at the salient angles, its sign changes to the opposite sign along the line where the rings and rod meet, and it is close to zero in the central part of this zone. A practically uniaxial tensile stressed state occurs in the middle of the core.

Thus, in the central part of the rod the direction of the fibers of the composite material should be arranged along its axis. Here the stressed state is always close to uniaxial (extension or compression). During compression of the rod, however, there is a danger of stratification of the unidirected composite material. To prevent it, the central part of the zone of contact between the core and ring should have binding fibers in a transverse direction.

Answering the question of the structure of the composite material of the rod in the zone where it joins the rings is more complicated. Here the stresses change their sign and location during extension and compression of the connecting rod. A unidirected composite material is thus unsuitable here. Its fibers do not coincide with the trajectories of the main stresses in the connecting rod.

Neither is it easy to select the structure of the material of the encompassing belt since it receives stresses with different signs along its line of contact with the rings. This necessitates locating some of its fibers along the tangent to the ring in a zone in which the sign changes.

In view of what has been said above and also considering the technological capabilities for the manufacture of composite materials, the most feasible design version of the connecting rod is that shown in Figure 1. This connecting rod consists of two metal rings (2 and 4) that

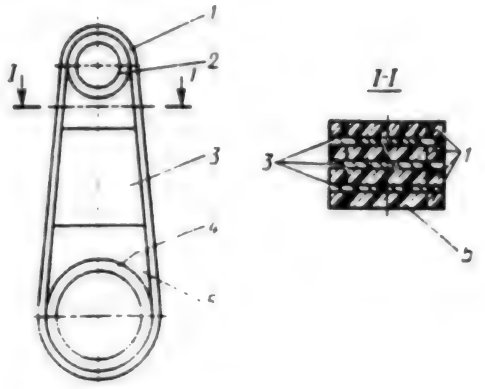

Figure 1

are glued to a rod (3) made of alternating thin composite bands, where the fibers of the base of the woven filler are parallel to the connecting rod's axis; reinforcing overlays (5) (they have a woven filler at a 45° angle to the axis); and a belt (1) made of unidirected composite material.

COPYRIGHT: Izdatelstvo "Mashinostroyeniye", "Avtomobilnaya promyshlennost",1990

UDC 621.43-034.13

Components Made of High-Strength Cast Iron

907F0314E Moscow AVTOMOBILNAYA PROMYSHLENNOST in Russian No 5, May 90 pp 14-15

[Article by V. A. Belov, A. V. Shlykova, and Ye. N. Lebedeva, Moscow Auto Mechanics Institute]

[Text] Numerous research projects conducted both in our country and abroad have shown that high-strength cast iron is practically equivalent to steel from the standpoint of its mechanical properties and even surpasses it from the standpoint of its casting properties.

These advantages are not achieved under all casting conditions, however. For example, a study of the operating practice of the plant Motordetal in Kostroma confirms that when internal combustion engine cylinder sleeves are manufactured by centrifugal casting, surface chill of the sleeves is frequently observed. The reason is the temperature of the molds (generally in the first two turns of the roundabout). Cases of poor contact of the refractory coating and the inner surface of the chill mold that lead to the introduction of quartz sand into the outer surface of the casting occur for the same reason. And while the chill can be eliminated by subsequent annealing, the abrasive material can only be removed by removing a layer of metal.

Eliminating these shortcomings and sharply reducing the consumption of metal-cutting tools for subsequent machining of the castings is possible by heating the chill molds and stabilizing the temperature conditions under

which they operate (both in the beginning of a shift and after idle times owing to different failures of the mechanical equipment). In view of this, the Moscow Auto Mechanics Institute developed and manufactured a unit to heat chill molds during centrifugal casting of sleeves on rotary machines at the plant Motordetal in Kostroma.

The most serious shortcoming of producing sleeves by the centrifugal method of casting is, however, the liquation of phosphorus, carbon, and silicon to the outer surface of the sleeve; this reduces the hardness of the inner working surface of blanks made of ordinary gray cast iron, which is impossible to eliminate (it is determined by the very essence of the casting method). The Moscow Auto Mechanics Institute therefore tested the possibility of manufacturing sleeves from high-strength cast iron by a modification of gray cast iron. The research conducted showed that this approach is justified. The formation of ball-like or a vermicular form of graphite begins with the outer surface of the sleeve (where the cooling speed is greatest) and ends on the inner surface. Therefore, with an optimal metering of modifier it is possible to obtain a uniform form of graphite along the entire cross section of the casting. In addition, by using complex modifiers containing (besides rare earth metals and magnesium) significant amounts of silicon, it is possible to create a high-silicon ferrite layer with increased hardness (unlike the ordinary ferrite on sleeves made of gray cast iron during centrifugal casting) on the sleeve's inner surface. Overall, the technology for producing sleeves from high-strength cast iron during centrifugal casting that was developed at the institute made it possible to stabilize the hardness of the sleeves along their cross section both before and after heat treatment, reduce the allowances for machining the sleeve's internal surface, and avoid chill on the sleeve's inner surface.

Also of great interest (in addition to the aforementioned) are those developments of the Moscow Auto Mechanics Institute related to selecting material for the chill molds of centrifugal machines operating under conditions of diverse effects (centrifugal forces, pressure of the metal poured into the mold, and above all uneven and repeated heating of the ingot molds). Therefore, one of the main indicators of a material's suitability for chill molds is its heat fatigue strength. Research on this indicator conducted on different grades of cast iron confirms that the decisive factors affecting heat resistance are the form and distribution of the graphite.

Ring pots may also be cast from high-strength cast irons, in view of which the Moscow Auto Mechanics Institute developed a technology for manufacturing them from high-strength cast iron with a ball-like or vermicular form of graphite by casting in sand molds and by the centrifugal method.

COPYRIGHT: Izdatelstvo "Mashinostroyeniye", "Avtomobilnaya promyshlennost",1990

Effectiveness of Two-Loop Intake System in Internal Combustion Engine

907F0314D Moscow AVTOMOBILNAYA PROMYSHLENNOST in Russian No 5, May 90 pp 13-14

[Article by B. S. Stefanovskiy, doctor of technical sciences, A. T. Reppikh, and R. K. Gadelshin, Melitopolsk Institute for Mechanization of Agriculture]

[Text] As is known, motor vehicles' fuel consumption decreases if the fuel-and-air mixture is heated. It is also known, however, that when the intake line is throttled, the degree of heating is sharply reduced with all of the ensuant consequences for fuel consumption.

One method of avoiding this shortcoming is to feed the mixture along channels (having reduced cross sections) heated by the exhaust gases in low-load modes and to feed it along channels with an increased cross section and with an adequate degree of warming by the coolant during large openings of the throttle.

Such a system was developed and tested in an engine with a working volume of 1,090 cm^3 both on a stand and on the road.

As a result, it was established that the optimized intake system significantly (up to 50 g/kWh) reduces the specific effective fuel consumption at crankshaft rotation frequencies of less than 3,500 and more than 5,000 min^{-1}. In the range between 3,000 and 5,000 min^{-1}, consumption turns out to be close (differing by 1-3 g/kWh) to that in the case of a series-produced system. In an engine with an optimized intake system, however, the filling of the cylinders is worsened somewhat, and for this reason the power (by 0.5 kW) and torque (by 2.5 N x m) are reduced throughout nearly the entire rotation frequency range. The exception is modes corresponding to frequencies below 2,000 min^{-1}. Here, when an optimized intake system is used, the power and torque increase by nearly the same amount.

The following advantage appeared in the optimized intake system: it gives the engine the capability of operating on a poorer mixture, which is the equivalent to a reduction in specific effective fuel consumption by 10 to 15 g/kWh. And it is characteristic that an optimized system yields a fuel consumption corresponding to the regulation limit for a series-produced system over a rather wide range of operating modes.

The nature of the heating of the intake line's wall in the zone of separation of the flow of mixture under the carburetor when the vehicle is in a steady motion was also investigated. It turned out that in the optimized intake line the temperature was 35-40 K lower than in a series-produced line. Because of the more intensive heating of the mixture, the operating fuel consumption was reduced by 0.1 to 0.25 l/100 km, or 2.5-4 percent, at speeds of 70 to 110 km/h. At speeds above 110 km/h, the series-produced system provided a gain of 0.2 l/100 km; however, at speeds of more than 130 km/h it provided a

gain of up to 0.8 l/100 km, and the maximum speed was 2.25 km/h higher with a series-produced system.

Table 1 presents the results of a comparison of the dynamic qualities of a motor vehicle equipped with test and series-produced systems.

Table 1.

Acceleration Conditions	Acceleration Time, s, With Intake System:	
	Series-Produced	Optimized
0-100 km/h	16.7	18.6
0-400 m	20.0	20.85
0-1,000 m	37.8	39.5
40-100 km/h (fourth gear)	29.6	31.66
40-100 km/h (fifth gear)	39.6	44.4

As is evident from Table 1, the optimized intake system diminished the vehicle's dynamic qualities somewhat. This fact was confirmed during a stand test with race drums. It became clear, however, that the main reason is a 0.2- to 0.5-second increase in the delay from the moment when the throttle valve is opened to the beginning of the vehicle's increase in speed that occurs in the optimized system. After the capacity of the carburetor's acceleration pump was increased, however, the vehicle's dynamics were restored in second gear, and in the third and fourth gears the acceleration time became even lower than in the series-produced system (by 1.4 seconds).

The dynamic qualities of a vehicle with an optimized intake system may thus be normalized by selecting the acceleration pump's capacity. But this does not reduce the vehicle's fuel economy and the toxicity of its exhaust gases.

With respect to the operating fuel expenditures, the tests yielded the following results. In accordance with a pure city cycle, the optimized intake system reduced fuel consumption by 5.4 percent with a simultaneous reduction in maximum toxicity (respective reductions of 2.4 and 4.28 g/test or 17 and 41 percent for carbon oxides and hydrocarbons).

Table 2 presents the data obtained for the steady speeds characteristic for city conditions.

Table 2.

Intake System	Vehicle's Speed, km/h	Gear	Fuel Consumption, kg/h	Exhaust Gas Components		
				Carbon Oxides, %	Hydrocarbons, ppm	Rarefaction Behind Throttle Valve, kPa
Optimized	15	I	1.14	0.25	300	60
	32	II	1.55	0.2	250	57
	50	III	1.79	0.2	210	51
Series-produced	15	I	1.16	1.05	250	67
	32	II	1.61	0.5	250	61
	50	III	1.83	0.25	250	53

The wall temperature of the optimized intake system reached 370-380 K (100-110°C) during operation in accordance with a city cycle. Because of this and a reduction in the rarefaction behind the throttle valve, the fuel consumption at characteristic speeds in the optimized intake system was 2 to 4 percent lower with a simultaneous reduction in the content of toxic components in the exhaust gases.

Overall, it may be said that the optimized intake system provides a perceptible fuel savings in all of a vehicle's operating modes. The insignificant reduction in power and torque noted during the tests have no significance and, when necessary, may be compensated for when finalizing the system.

COPYRIGHT: Izdatelstvo "Mashinostroyeniye", "Avtomobilnaya promyshlennost",1990

UDC 629.113-598

Antilocking Systems and Brake Drive Operation

907F0314C Moscow AVTOMOBILNAYA PROMYSHLENNOST in Russian No 5, May 90 p 13

[Article by A. M. Galaktionov and V. V. Poluektov, NIIAE [not further identified]

[Text] The quality of the operation of antilocking systems is assessed primarily by two criteria—stability and braking distance, which are determined by the overall dynamics of the system regulating the brake drive, namely, by the brake drive itself. The point is that the time required for its activation is the limiting node from the standpoint of the speed of the entire system and, consequently, the quality of the antilocking system's operation.In fact, time delays

in two other components of the control system, i.e., the control unit and actuator (modulator), are not large, amounting to 5-10 and 10-12 ms, respectively. The inertia (time constants) of the nodes of a pneumatic brake drive are much larger. For example, the time constants of the braking chambers of different modifications of ZIL, KamAZ, and MAZ vehicles (vehicles produced respectively by the Moscow Automotive Plant imeni I. A. Likhachev, the Kamsk Automotive Plant, and the Minsk Automotive Plant) are 70-200 ms, whereas those of the braking mechanisms are 90-130 ms.

The question arises as to whether such a system is effective enough to prevent locking of the wheels. Indeed, as practice has shown, even short-term (50 to 70 ms) locking of the wheels of an automatic brake system during braking on a surface with low cohesion properties may result in a loss of course stability.

To answer the question posed, specialists from the NIIAE conducted research with a computer. To evaluate the operating quality of the antilocking system installed in an MAZ-5336 vehicle, they selected the worst scenario from the standpoint of control during braking, i.e., the transition from dry asphalt concrete pavement to ice (cohesion coefficients of 0.7 and 0.2, respectively).

It was established that significant "drops" in the speed of the wheels relative to that of the vehicle develop for the given vehicle, which has a significant brake drive inertia (time constants of 0.2 s for the brake chamber and 0.11 s for the brake mechanism and a hysteresis of 40 percent). These drops result in a reduction in the control frequency and, consequently, in a reduction in the cohesion utilization factor.

As modeling of the process of braking with an antilocking system has shown, satisfactory results in the given cases can only be obtained with brake chamber time constants not exceeding 70 ms and with a hysteresis of not more than 10 percent.

Having an antilocking system operate effectively thus requires improving the brake drive. Otherwise vehicles will not only not meet the requirements stipulated in United Nations Economic Commission for Europe Rule No 13 but will also discredit the very idea of equipping vehicles with antilocking systems. All of this must naturally be considered back in the stage of designing vehicle brake systems.

COPYRIGHT: Izdatelstvo "Mashinostroyeniye", "Avtomobilnaya promyshlennost",1990

UDC 621.43-523.8:681.325.5-181.4

Architecture of Internal Combustion Engine Microprocessor Systems

907F0314A Moscow AVTOMOBILNAYA PROMYSHLENNOST in Russian No 5, May 90 pp 9-11

[Article by A. K. Giryavets, V. V. Muravlev, and V. N. Tupikin, Central Automobile and Automotive Scientific Research Institute]

[Text] The past few years have been characterized by the rapid penetration of electronics into engine control systems. In its initial stage, their introduction followed the path of simple replacement of mechanical devices and regulators by their electronic analogues. This replacement permitted more precise engine control and made it possible to keep engines in operation longer and reduce their toxic emissions and fuel consumption. But electronics developed. And in the next stage in this development came digital and then microprocessor control systems and finally unified integrated internal combustion engine microprocessor control systems.

Analysis of the structure of these systems confirms that sensors are practically always the primary information sources, i.e., sensors of absolute pressure in the intake system or mass air consumption, air and coolant temperature, position of the throttle valve, position of the engine's crankshaft and the camshaft, and the presence of oxygen in exhaust gases and detonation. Systems control the ignition advance angle, the duration and moment of fuel supply, the valves for additional air feed and recirculation of exhaust gases, and the starter, fuel pump, etc. Software makes it possible to identify an engine's operating mode and process incoming information in accordance with algorithms corresponding to each of the modes. The laws governing engine control (the dependencies between the sensors' signals and the required settings issued along the control channels) are stored in the control system in the form of tables or functional dependencies. The latest control system prototypes have program adaptation equipment providing the capability of considering a change in external conditions and the characteristics of the control object.

The foundation of the integrated internal combustion engine microprocessor control system are control algorithms implemented in software. The electronics of the control unit enables these algorithms to function with minimum hardware expenditures. It is obviously that when the electronics are developed, the main problems to be resolved are the control system's structure (selection of the sensors, control channels, and actuators), identification of the information streams and principles

of processing them, and separation of the signal processing algorithms into hardware and software. These are the tasks entailed in selecting the system's architecture.

Just as obvious is the fact that this architecture should be determined by a minimum of three factors: the nature of the operational processes occurring in the engine, the maximum length of the information processing cycle, and the frequency with which control instructions are issued to the actuators.

We will examine these factors.

The actual processes occurring in internal combustion engines may be divided into three groups: those determined by the crankshaft's rotation frequency; those that do not depend on it but are caused by a change in the control and destabilizing effects and the mechanical and thermal inertia of the engine; and those that are connected with the aging and wear of the engine, the sensors, and the control system's actuators as well as by a change in operating conditions. In other words, the engine may be looked upon as an information source with three groups of signals that differ from the standpoint of their time characteristics.

To put it more specifically, the first group may include cyclic gas dynamic processes in the intake system that are connected with gas exchange, processes of formation of a fuel film in the intake systems upon a situational change in the engine's operating mode, processes of spark formation and fuel supply (for engines with distributed fuel injection); and the moment of the appearance of detonation in the combustion chamber. In reality, they are all uniquely connected with the angular position and rotation frequency of the engine's crankshaft. This means that their characteristics in the readout system, which is connected with the position of the crankshaft, remain constant, and if they are described as a function of the crankshaft's angular position, hardware and software implementation of the processing algorithm is greatly simplified.

The second group includes the following: the control effects of the driver; the change in load on the engine caused by a change in road conditions; gas dynamic processes in the intake system caused by displacement of the throttle valve; a change in the duration and moment of fuel supply and control of the ignition advance angle, including a reaction to the occurrence of detonation; and phenomena connected with the engine's thermal inertia, its cooling system, and its sensors and actuators. None of these processes depends on the rotation frequency or position of the crankshaft. The cycle of processing information connected with them may therefore be fixed with respect to duration.

The third group is connected with phenomena caused by the wear and aging of the engine, sensors, and actuators and with a change in the climate conditions in which the vehicle is operating, the characteristics of the fuel used, etc.

It follows from what has been said that a system controlling the operating process of a gasoline engine that considers its distinctive features most completely should be a computer based on separate processing of two information streams—synchronized with the position of the crankshaft (signals of processes in the first group) and realtime streams (signals of the processes in the second and third groups). The computers corresponding to them may be termed a synchronous processor and a real-time processor.

This subdivision not only makes it possible to minimize hardware expenditures but also makes it possible to significantly reduce the amount of software.

We will examine both types of processes.

Since a synchronous processor processes information related to the crankshaft's angular position, the duration of the processing cycle is, as was mentioned above, singularly determined by the position of the crankshaft and is constant in its coordinates. Its limit allowable maximum value depends on the spectral characteristics of the input signals and, according to our estimates, may range from 8 to 15 degrees p. k. v. [not further identified, possibly "of the crankshaft's position"]. This means that the cycles should be synchronized with the crankshaft's position with an interval of no more than 8 to 15 degrees p. k. v.

Signals from the sensors indicating the top dead center, the crankshaft's position, the crankshaft's angular position, the mass air consumption (or pressure in the intake line), and the detonation (of the detonation identification device) serve as the primary information needed to operate the synchronous processor. It also receives signals from the real-time processor regarding the required moment of the beginning of fuel supply and its magnitude. The processing of the input signals entails linearization and filtration of the signal from the sensor indicating the mass air flow rate for the sensor indicating absolute pressure in the intake line, correcting the duration of the fuel supply in accordance with the intake system's transfer characteristics (dynamic correction of the fuel supply) separately for each of the engine's cylinders, and conditioning of synchronization signals (for the detonation identification device, the device to control the ignition advance angle, and the device controlling the moment of fuel supply in the case of phased distributed fuel injection). The functions of the synchronous processor may also include diagnosis of the primary sensors and processor of any soft failures that occur.

The synchronous processor not only receives information but also sends it to the real-time processor (information regarding the ongoing mass air consumption, the nature of any error that arises, and signs of the occurrence of detonation in an individual cylinder).

As was said above, the second and third groups of processes do not depend on the crankshaft's position; they may all therefore be processed by a real-time processor. The maximum duration of the information

processing cycle is determined, on the one hand, by the frequency characteristics of the instructions from the drier and, on the other hand, by the maximum possible rate of change in the engine's operating mode. Analysis has shown that the frequency range of instruction signals does not exceed 16 to 20 Hz, whereas the frequency of a change in control instructions given the maximum possible rate of change in the engine's state does not exceed 20 to 50 Hz depending on the type of engine. Hence follows the possibility of using a fixed duration of the information processing cycle in the real-time processor. Moreover, since information is input at specific moments in time, measurement of the time intervals may be replaced by simply counting the number of sampling cycles. This in turn makes it possible to greatly simplify the measurement and formation of time intervals; simplify measurement of the frequency, acceleration, and unevenness of the rotation of the crankshaft; as well as simplify the operations of integration and differentiation. Moreover, the information processing cycle becomes independent of the specific branch of the algorithm.

The duration of the real-time processor's information processing cycle, which is specified by the operating period of a system timer, should amount to about 20 ms. Protection against soft failures requires a protection system with program dumping that restarts the real-time processor in the event of the absence of an interrupt instruction in the running information processing cycle.

As its information source, the processor uses data formulated by the synchronous processor (the running mass air flow rate or absolute pressure in the intake system or a sign indicating detonation in an individual cylinder) and real-time signals produced by polling the timer of the crankshaft's rotation frequency and the sensors characterizing the instructions of the driver (such as the position of the throttle valve, activation of the starter, etc.), the engine's temperature status, the oxygen content in exhaust gases, etc.

The real-time processor controls the engine either through the synchronous processor (the moment and amount of fuel supply) or by formulating instructions directly to the actuators controlling the ignition advance angle in each of the engine's cylinders (with an allowance for detonation) and to the actuators controlling the feed to additional air, the valve recirculating exhaust gases, and the relays controlling the starter, the fuel pump, heating of the sensor indicating the oxygen content in the exhaust gases, etc.

For high-quality engine control, the microprocessor system should be capable of changing its parameters and the structure of its control algorithm. This is manifested in a change in both the ultimate control objectives and in the constraints, which depend on the engine's operating mode and are implemented by software. The latter consists of two functionally different parts: the nucleus and the superstructure. The nucleus performs the function of control regardless of either the engine's operating mode or the rotation frequency of its crankshaft. It measures and processes the sensors' signals. After ultimately receiving the values for the running cylinder fill cycle, it compares them with the values fixed in the base tables and issues control instructions to the actuators. These instructions ensure the optimum change in the engine's operating mode (including without detonation).

The superstructure formulates the structure of the algorithms and program controllers (or versions of the base tables). Its foundation is a program called "Dispatcher", which analyzes the engine's current and preceding status, identifies its operating modes, and selects one branch or other of the control algorithm.

Everything stated above with respect to the real-time processor also applies to the second group of processes in an internal combustion engine. As far as the third group is concerned, the control system there must itself adapt to the internal combustion engine's changing operating conditions. This is accomplished by introducing additional sensors and forming feedback circuits encompassing the control system as a whole.

Hardware implementation of the internal combustion engine microprocessor control system architecture under examination is determined by the speed of the microprocessors used. If the mean time required to implement an arithmetic instruction ranges from 0.5 to 1 μs, both processors may be based on a single microprocessor that divides its operating time by using a system of interrupts from the signals indicating the angular markers of the position of the crankshaft and the system timer. At a lower speed it is necessary to use two microprocessors, i.e., to use hardware separation of the functions of the real-time and synchronous processors. But this type of structure requires creating a common memory region accessible from both microprocessors.

The architecture of the construction of an on-board microprocessor control system examined best meets the requirements stipulated for such a system for an automotive engine, including from the standpoint of universality of application and control quality.

COPYRIGHT: Izdatelstvo "Mashinostroyeniye", "Avtomobilnaya promyshlennost",1990

UDC 629.113-592.001.63

Ergonomic Properties of Systems

907F0314B Moscow AVTOMOBILNAYA PROMYSHLENNOST in Russian No 5, May 90 pp 12-13

[Article by O. V. Mayboroda and V. V. Savelyev, candidates of technical sciences, NITsIAMT [not further identified], Siberian Highway Institute]

[Text] Traffic safety in a deceleration mode is determined by a number of properties of the vehicle itself and its brake system: course and trajectory stability margins (their presence permits fuller realization of maximum

deceleration); the brake system's power, i.e., the maximum deceleration that it can provide; and its ergonomic properties, which make it possible to follow the braking specified by road conditions and to regulate it when it is restricted by stability constraints. The first two of the properties listed are measured rather precisely. As far as the third is concerned, it has not actually been investigated. For this reason there is still no description of a braking system as a servo control system, and there is almost no research on the process of braking in the closed system "driver-vehicle."

In fact, during the process of moving, to ensure his safety, the driver continually assesses the road situation by comparing distances to other participants in the traffic with the "standard" distance, i.e., what in his view is necessary to reduce his speed to a safe one. And if he discovers that he must reduce his speed, he moves the brake pedal and regulates his position such that the deceleration deviates as little as possible from the mean for the specified braking distance. In the case of skidding or drift, he must also correct the braking force to create a cohesive force margin in the transverse direction and ensure the vehicle's course or trajectory stability. Because of this, the increase in the braking distance will be even larger as the braking force decreases when compared with the maximum possible force from the standpoint of the criterion of course and trajectory stability. (If the necessary course stability margin is provided by the braking force regulator in the rear wheels, the size of the braking distance will depend on how precisely the driver can regulate the braking force relative to the maximum according to the m-S diagram). When the vehicle has an antilocking system, the driver is relieved of the necessity of controlling the braking force in order to create the required cohesive force margin. This system cannot, however, guarantee the smoothness of a change in deceleration with standard brakes. In addition, if the driver does not have the capability of smoothly regulating the braking force, the antilocking system will be activated more frequently than necessary, which will lead to increased wear of the components of the system itself, the tires, and the running gear portion of the vehicle. The antilocking system also affects the driver himself: if he has operated a vehicle equipped with an antilocking system for a long period of time and the latter fails on a slippery road, he may turn out to be in a helpless situation if the brake system does not possess servo action.

What has been said proves the following: good ergonomic properties, i.e., those that permit the driver to regulate the braking force in accordance with the task being performed, are no less important than is brake effectiveness.

We will examine the functioning of the system "driver-vehicle" during the braking process.

Having decided to reduce the speed to one that is safe for the given road situation, the driver subconsciously programs his actions: they are specified by the required amount of deceleration, the movement of the brake pedal, and the force on it. He then implements the braking, during the course of which he continuously compares the results achieved with the program and, when necessary, corrects his actions. He uses two feedback channels—an external channel (information about the speed, deceleration, and distance remaining to the obstacle), according to which he assesses the result of his control, and an internal channel (movement of and force on the pedal), according to which he determines the movement of the pedal and predicts the amount of deceleration corresponding to the movement of the pedal since information is transmitted along the internal feedback channel at a speed of 0.04 s and along the external channel within 0.1 to 0.2 s, i.e., with a delay of 0.06 to 0.16 s. Internal feedback increases the precision of regulating deceleration under the condition that the movement of the pedal and the force on it are adequate to the anticipated braking of the automatic brake system. In other words, these indicators correspond to the standards embedded in the driver's memory. Otherwise, the deceleration observed will not conform to the anticipated characteristic, and the driver will need to correct his program based on feedback, which diminishes the quality of the braking process.

Can this be avoided, i.e., can a situation be achieved in which the driver can always best use his internal feedback? This question can be answered by examining the static characteristic (Figure 1) describing the feedforward and feedback of the brake system as a servo control system. The braking force coefficient has been taken as the "output" of the brake system since, while controlling the deceleration, the driver regulates the braking force. The magnitude of the control effect is, however, determined not by its absolute value but by its relative value, which equals the ratio of the braking force to the vehicle's mass, i.e., the braking force coefficient q_T.

The optimum interaction between the driver and the brake system is achieved when the dependencies presented in Figure 1 are selected when the brake system is designed with an allowance for the distinctive features of man's perception of information. The generalized psychophysical law establishes two types of dependencies between the intensity of stimulation and the intensity of the evoked perception: power and logarithmic dependencies.

The research conducted makes it possible to conclude the following: the characteristic "pedal movement-braking force coefficient" located in the first quadrant, which describes the sensitivity to control, should be expressed in terms of a power function. The characteristics "pedal stiffness" and system "reactivity," which are located in the fourth and third quadrants respectively, should be expressed by logarithmic functions (the characteristics corresponding to these requirements are shown by solid lines). The curve of the change in the braking force coefficient q_T along the pedal's course L should pass through the point C, the size of the insensitivity zone L_0 should not exceed 12 mm, the effective

pedal course (L_{max} - L_0) should lie in the range from 40 to 100 mm, and the hysteresis b_L should equal 10 mm. The standard appearance of this curve in domestic and foreign vehicles tested does not meed ergonomic requirements (it is shown by broken lines in Figure 1).

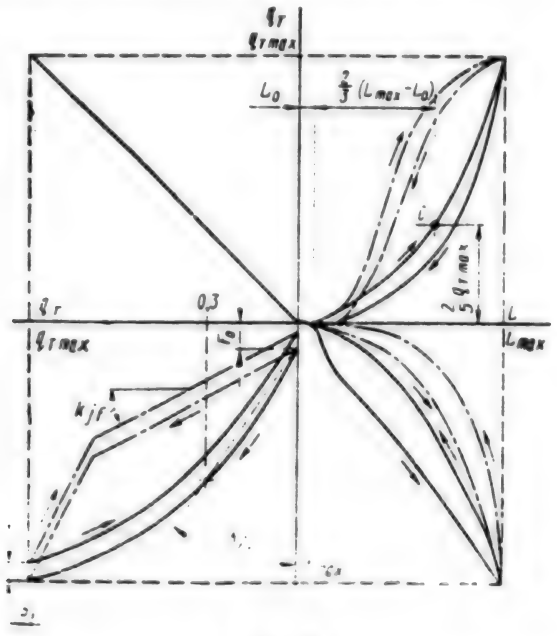

Figure 1

The characteristics pedal "stiffness" and system "reactivity," which are shown respectively in the fourth and third quadrants, describe the internal feedbacks. Test results show that the shape of these characteristics in vehicles tested does not meet ergonomic recommendations (the broken lines).

The specified dependencies are nonlinear. Describing and estimating them requires examining their specific parameters. The "threshold" of the force F_0 in the characteristic "reactivity" is the most important ergonomic parameter. It should be no less than 45 N, i.e., it should be sufficient to balance the mass of the foot. At the same time, the "threshold" for automatic braking systems in categories M_1, M_2, and N_1 should not be greater than 60, whereas that for categories M_3, N_2, and N_3 should not be greater than 75 N. If these values are exceeded, the driver perceives a "seizing" of the pedal at the initial moment.

As the pedal moves further, its elastic resistance to movement gives the driver an advance sense of the magnitude of the deceleration provided the nature of the build-up of force meets ergonomic requirements. The required rate of build-up in force given the increase in deceleration described by the conversion factor k_{jF} is related to the magnitude of the "threshold" force. It has been established experimentally that the ratio F_0/k_{jF} must be no less than 0.23, i.e., when the "threshold" increases, so too should the "reactivity" and vice versa. To determine k_{jF} when the dependence is nonlinear it is necessary to pass the vertical through the point corresponding to the braking force coefficient q_T = 0.3, as is shown in Figure 1.

The third main point of the dependence, i.e., the magnitude of the hysteresis b_F (it allows for dry friction in the system and must not exceed 40 to 60 N) corresponds to the maximum force on the pedal (F_{max}) at which the driver can fully realize the vehicle's braking properties. This force equals 300 N for automatic brake systems in categories M_1 and M_2, 350 for those in category M_3, and 400 N for those in category N, whereas it must be no less than 200 N since it would not be able to ensure the required value of k_{jF}.

The dynamic properties of braking systems are described by two sequentially connected standard nodes assumed in automatic control theory: the node of pure delay by the time τ and the aperiodic first-order node with the constant time T. The dynamic and static properties of a vehicle's brake system are interconnected. The point is that at high τ and T (a large delay in the suppression of braking force) and low "reactivity" k_{jF} (low rate of build-up of force on the brake pedal), the driver pressing on the pedal and thereby increasing the force on it does not receive adequate information regarding the magnitude of deceleration occurring within the time τ + T. He therefore continues to move the pedal until information is obtained along the external feedback channel, which results in "overbraking." This is characteristic for vehicles with a pneumatic brake drive, in which the delay for moving the pedal is large and which means that, for them, k_{jF} should be larger than in the case of a hydraulic drive.

Using a vacuum amplifier in a hydraulic brake drive may also change the properties of the latter. Research conducted on a specific prototype automatic braking system showed that connecting an amplifier increases τ and reduces T. T even assumes negative values since the rate of the build-up of pressure in the system outpaces the speed of the pedal's movement. From the standpoint of the principles of automatic control theory, this means that the system's structure changes as follows: instead of an aperiodic node, a boosting node appears in it. In addition, the amplifier also worsens the static characteristic, transforming it from concave (the recommended characteristic) to convex; consequently, the precision of braking regulation is reduced.

Even a fleeting glance at the characteristics of controlling brake systems thus shows that the driver's ergonomic requirements are clearly not considered sufficiently when they are designed, not to mention when systems with previously specified ergonomic properties are created. And indeed this is a very significant reserve for increasing the safety of automatic brake systems that must not be ignored, including from the standpoint of the competitiveness of our automotive technology.

COPYRIGHT: Izdatelstvo "Mashinostroyeniye", "Avtomobilnaya promyshlennost",1990

UDC 621.9.015.7.001.5+621.793

Effect of Structural Condition of Coating on Performability of Cutting Tools

907F0305I Moscow IZVESTIYA VYSSHIKH UCHEBNYKH ZAVEDENIY: MASHINOSTROYENIYE in Russian No 3, Mar 90 pp 136-139

[Article by V. V. Letunovskiy, candidate of technical sciences and docent, A. V. Petruchenya, assistant, V. B. Yasinskiy, assistant, and N. A. Savenko, engineer; first paragraph is IZVESTIYA VYSSHIKH UCHEBNYKH ZAVEDENIY: MASHINOSTROYENIYE abstract]

[Text] This article shows the effect of the conditions of the application of a TiN coating on the level of internal friction and performability of cutting plates made of the hard alloy T14K8. The interconnection of the acoustic emission characteristics and the cutting plates' wear parameters is investigated. An indirect criterion for determining the thickness of coatings, i.e., the amount of internal friction, is proposed.

A set of criteria—coating thickness, strength of the bonding of the coating to the base, microhardness, buckling strength, and other indicators—are used to evaluate the quality of coatings on cutting tools.[1,2] These indicators are frequently included in equations for optimizing the parameters of the cutting process when using hard alloy plates with coatings.[3] The large number of partial indicators makes it difficult to use an optimization model; consequently, it is necessary to find and validate new and more universal criteria for the performability of tools with coatings.

The effect of a coating's structural condition on cutting tools' performability has not been studied adequately. It has been shown[4,5] that the structural condition of a material and its performability given specified performance conditions is conveniently characterized by the level of internal friction—an integral quantity that is specified in terms of the damping factor of elastic vibrations and related to the specific surface of the intergrain and interphase boundaries, chemical composition, presence of pores, dislocations, and other defects in the tool material.

The effect of the conditions of applying a TiN coating on the level of internal friction and the performability of cutting plates of the hard alloy T14K8 was studied, and the interconnection of the cutting plates' performability and the acoustic emission characteristics has been established.

In the cutting plates studied, the level of internal friction was measured by a UVT-6 ultrasound structural analyzer before application of a coating in order to determine the spread of the internal friction values within the limits of one batch of 64 plates.

The plates were divided into two batches based on their level of internal friction. The first batch included plates with an identical initial level of internal friction, which assumes the identical structural heterogeneity of the material of the base. A TiN coating was applied to these plates by the KIB [not further identified] method on a Bulat-3 unit in the following modes: ionic cleaning (with a pressure in the vacuum chamber of 1.33 MPa, an accelerating voltage of 1,000 to 1,500 V, an arc current of 75 to 80 A, and a temperature of the machined surface between 550 and 600°C) and precipitation (with a pressure in the working chamber of 1.33 MPa, a nitrogen pressure of 0.9 Pa, a base voltage of 150 V, and an arc current of 75 to 80 A). To produce coatings with different thicknesses, spraying times of 2, 4, 6, and 8 hours were used.

The second batch included plates with minimal, average, and maximum levels of internal friction. Eight hours was required to apply coatings to the plates in this batch. Identical modes of applying coating on the specimens in both batches were adopted.

A control batch of plates with minimal, average, and maximum levels of internal friction was also selected. No coating was applied to these plates. They were intended for comparative durability tests.

The durability tests were conducted during sharpening of the alloy KhN77TYuR with a constant cutting speed of V = 1.9 m/s, a feed of S = 0.25 mm/rotation, and a cutting depth of t = 0.5 mm on a 16K20 machine tool equipped with a device to record the acoustic emission. During the process of the durability experiments, acoustic emission spectra were recorded by using an SK4-59 spectrum analyzer, and the wear face on the main flank surface was measured. Next, the dependence of the change in the wear face f, the pulse amplitude of the acoustic emission Ai, and the area of the acoustic emission spectra ΣF on the coating thickness d was measured along with the interconnection between the wear ends and the acoustic emission characteristics.

Fractographic studies of the coating surfaces, the tool's fracture zone, the transition zone, and the coating thickness were conducted by using an REM-100U scanning electron microscope.

Measurements of the magnitude of the internal friction in the plates before the coating was applied showed that the level of internal friction in the batch of plates studied varied from $3.3 \cdot 10^{-5}$ to 5.5×10^{-5}. The spread of internal friction values is explained by the structural inhomogeneity of the cutting plates that occurred in the process of their manufacture.

After application of the coating, the internal friction increased by a factor of 1.1 to 1.8. The spread of internal friction increased in the specimens in the second batch. The internal friction varied from 3.5×10^{-5} to 8.2×10^{-5}. The increase in the internal friction is explained by the inhomogeneity of the product that arises during the

process of applying the coating, in whose structure pores, microcracks, stratifications, and other defects form.

Direct measurements have established that the coating thickness in the specimens in the first batch varied from 4 to 8 μm as a function of spraying time, whereas in the specimens in the second batch it amounted to 7-8 μm.

Investigation of the level of internal friction in cutting plates with an identical initial level of internal friction showed that as the coating thickness increased from 4 to 8 μm, the internal friction decreased from 5.8 x 10^{-5} to 3.9 x 10^{-5} (Figure 1).

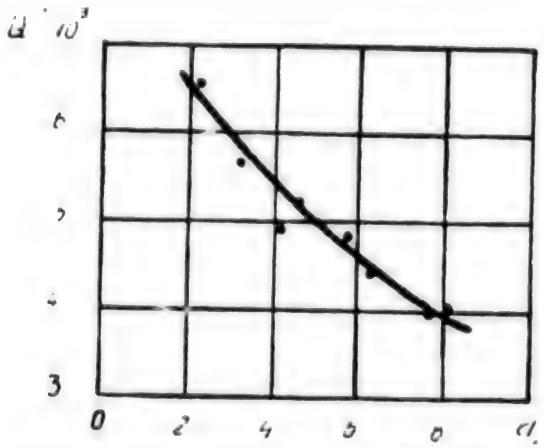

Figure 1. Internal Friction Q^{-1} as a Function of the Coating Thickness d

The higher level of internal friction of the plates with the lesser coating thickness is explained by the decisive effect of the transition layer and the small thickness of the quality layer of coating. The transition layer contains pores, oxides, and carbide and nitride inclusions, which increase with the level of internal friction in the plates with coatings.

Figures 2 and 3 present the results of the durability tests.

The experimentally obtained acoustic emission spectrum reflects the development of the tool's wear and breakdown. The amplitude of the characteristic peaks characterizes the energy intensity of the chip formation process, and the area of the spectrum is connected with

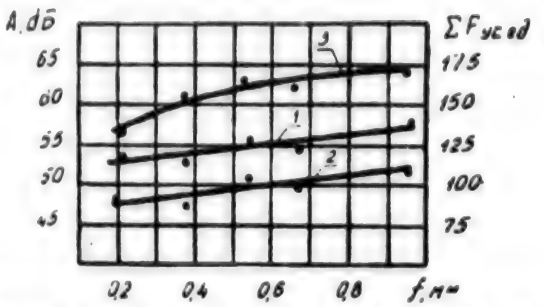

Figure 2. Amplitude of the Signal Ai (1, 2) and Area of the Acoustic Emission Spectra F (3) as a Function of the Wear Face f; Frequency, kHz: 1, 35-70; 2, 70-100

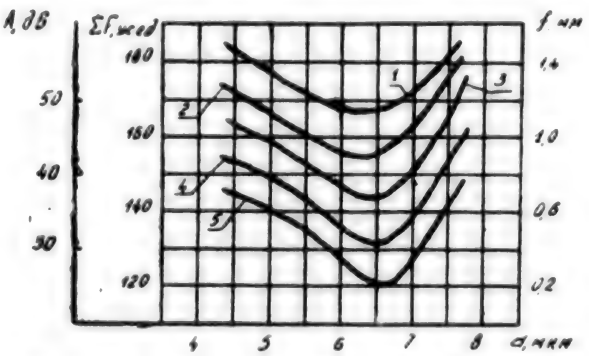

Figure 3. Amplitude of the Signal Ai (1, 2, 3) of the Area of the Spectra F (4) and Wear Face f (5) as a Function of the Thickness of the Coating d: Frequency, kHz: 1, 70-100; 2, 110-150; 3, 150-200. (F is plotted in arbitrary units, and d is plotted in μm.)

the energy expended on elastic, plastic deformations and the breakdown of the tool material and the material being machined.[6]

The amplitude distribution of the acoustic emission signals was studied in the frequency range from 0 to 500 kHz. In this frequency range five characteristic peaks are constantly detected, both during the operation of cutting plates with a coating and those without one. The characteristic peaks during cutting by tools with a coating appear in narrower frequency ranges and are frequency shifted when compared with those of the tools without a coating (Table 1).

Table 1. Frequency (kHz) Range of the Amplitude Distribution of the Characteristic Peaks

Tool Material	Frequency of Characteristic Peaks, kHz				
	1	2	3	4	5
T14K8	0-30	30-70	70-120	120-180	180-250
T14K8 + TiN	0-30	30-60	60-100	100-140	140-180

A linear growth of the amplitude of the acoustic emission pulses as a function of the wear face in the second and third frequency ranges (Figure 2) was established during cutting by the tools with a coating. The correlation coefficients in the Ai-f pairs amounted to 0.91 in the interval from 30 to 60 kHz, 0.89 in the interval from 70

to 120 kHz, and 0.95 in the interval from 180 to 250 kHz. In other ranges the correlation is very weak or absent. The change in the frequency characteristics of the acoustic emission spectra is evidently related to the change in conditions of the tool's contact with chips and with the component being machined.

Fractographic analysis of the breakdown surfaces in coated and uncoated specimens showed that the principal wear is abrasive wear. The tool wears along both the face and flank surfaces. The formation of fatigue cracks close to the cutting edge is observed. Breaks and sinks in the cutting edges were established during the experiments. It thus follows that creep is one of the possible mechanisms of the breakdown of tools with coatings. Because of a reduction in the friction coefficient and the coating's adaptation to cutting conditions, the depth and spacing of the abrasive wear notches on the working surfaces is reduced.

The coating thickness affects the cutting tool's wear, which is reflected in the acoustic emission characteristics. It is evident from Figure 3 that a coating thickness of 6-7 μm corresponds to the minimum tool wear values, acoustic emission signal amplitudes, and energy expenditures. It should therefore be considered optimum. The greatest connection between the amplitudes of the acoustic emission signals and the coating thickness is observed in the frequency range from 30 to 140 kHz.

The coating thickness has a decisive effect on a cutting tool's performability since the coating prevents oxidation and thermomechanical breakdown and reduces adhesion of the tool material to chips. On the other hand, as the coating's thickness increases, its microhardness decreases, the number of defects increases, and the probability of the appearance of a hazardous defect that may lead to dynamic breakdown of the coating is increased.[1] Hence the connection between optimum coating thickness and the conditions of the cutting process.

Conclusions

The dependence of the amount of internal friction on the coating thickness that has been established makes it possible to use the level of products' internal friction as an indirect criterion for determining coating thickness.

For the hard tool alloy T14K8 with a TiN coating and for the machinable material KhN77TYuR, the optimum coating thickness is between 6 and 7 μm. It corresponds to the minimum tool wear.

The interconnection of the amplitude of acoustic emission signals, the area of the acoustic emission spectrum, and the wear of tools with a coating has been established. This makes it possible to use the acoustic emission method to monitor the condition of cutting tools with a coating and to determine their critical wear.

Bibliography

1. Vereshchaka, A. S., Tretyakov, I. P., "Rezhushchiye instrumenty s iznosostoykimi pokrytiyami" [Cutting Tools With Wear-Resistant Coatings], Moscow, Mashinostroyeniye, 1986, 192 pages.

2. Vlasov, V. M., "Rabotosposobnost uprochennykh trushchikhsya poverkhnostey" [Performability of Hardened Rubbing Surfaces], Moscow, Mashinostroyeniye, 1987, 304 pages.

3. Starkov, V. K., "Tekhnologicheskiye metody povysheniya nadezhnosti obrabotki na staknakh s ChPU" [Manufacturing Methods of Increasing Reliability of Machining on NC Machine Tools], Moscow, Mashinostroyeniye, 1984, 120 pages.

4. Letunovskiy, V. V., "Structure and Properties of Tool Steels," in collection "Fiziko-mekhanicheskiye i ekspluatatsionnyye svoystva instrumentalnykh i konstruktsionnykh materialov" [Physicomechanical and Performance Properties of Tool and Construction Materials], No 3, Krasnoyarsk, KPI, 1974, pp 3-17.

5. Letunovskiy, V. V., "Wear Resistance and Machinability of Metallic Materials," in collection "Fiziko-mekhanicheskiye i ekspluatatsionnyye svoystva instrumentalnykh i konstruktsionnykh materialov" [Physicomechanical and Performance Properties of Tool and Construction Materials], No 5, Krasnoyarsk, KPI, 1976, pp 63-67.

6. Podurayev, V. N., "Optimizatsiya protsessa rezaniya, rezaniye trudnoobrabatyvayemykh materialov" [Optimizatin of Cutting Process and Process of Cutting Hard-To-Machine Materials], Moscow, Vysshaya shkola, 1974, 589 pages.

COPYRIGHT: "Izvestiya VUZov. Mashinostroyeniye", 1990.

UDC 621.941.23-529:658.562.011.56

Investigation of Precision Characteristics of Feed Drives of Precision Lathe Modules

907F0305H Moscow IZVESTIYA VYSSHIKH UCHEBNYKH ZAVEDENIY: MASHINOSTROYENIYE in Russian No 3, Mar 90 (manuscript received 23 May 88) pp 132-135

[Article by B. M. Brzhozovskiy and M. V. Vinogradov, candidates of technical sciences, and A. A. Ignatyev, assistant; first two paragraphs are IZVESTIYA

VYSSHIKH UCHEBNYKH ZAVEDENIY: MASHINOSTROYENIYE abstract]

[Text] This article examines the precision of positioning the support of lathes in which different types of guides and drives are used.

The TPARM-100 module, which has gas guides in combination with a closed friction feed drive and laser interferometer, is examined.

The quality of shaping in precision machining, particularly under conditions of FMS technology using a small number of workers, is determined by the dynamic and static characteristics of the feed drives, especially by the precision and stability of positioning the end-effector during continuous and discrete feeds.

Other works[1,2] have examined the problems of the precision characteristics of feed drives. From the standpoint of their application in precision turning of small components under FMS conditions, however, they need to be examined in greater detail. The selection of the type of mechanical feed and control effects for the feed drive of a precision lathe module are substantiated below.

Existing feed drives cannot provide high parameters in view of their inherent features and shortcomings. A feed drive with a direct current motor and sliding guideways generally includes gear trains and a screw pair[3] that generally have gear ratio errors. In addition, at speeds below critical, relaxation vibrations are observed during which the maximum jump speed may be several times in excess of the average speed of movement. The general law is reduced to one where the magnitude of the dynamic error during positioning of the support is inversely proportional to the rigidity of the drive and directly proportional to the difference between the resting and motion friction forces. Obviously, the specified quantities have, in each case, fully specified values, and their effect cannot possibly be eliminated. Experimental data show that at speeds close to critical, the positioning error amounts to several micrometers owing to the discrepancy between the kinetic and static friction forces. Using stepping motors makes it possible to increase the precision of changing position at speeds below the critical on account of the fact that the instantaneous value of the velocity is much higher than its average value. It should be noted that in an open step drive, errors of the toothed, worm, and screw gear mechanisms account for a significant fraction of the error. Using a feedback sensor, for example, a laser interferometer with a readout discreteness of 0.3 μm,[5] makes it possible to compensate for static errors in mechanical gears. Figure 1a presents the results of measuring the precision of moving the support of a 16BO4P lathe equipped with an ShD5-D1 stepping motor with a worm reducing gear and a screw-slide nut pair with an open-loop control system. Figure 1b presents the results for a closed-loop system. It is evident from the graph that a closed-loop control system with a laser interferometer as the feedback sensor significantly reduces the effect of errors of the lead screw and reducing gear on the precision of positioning the support.

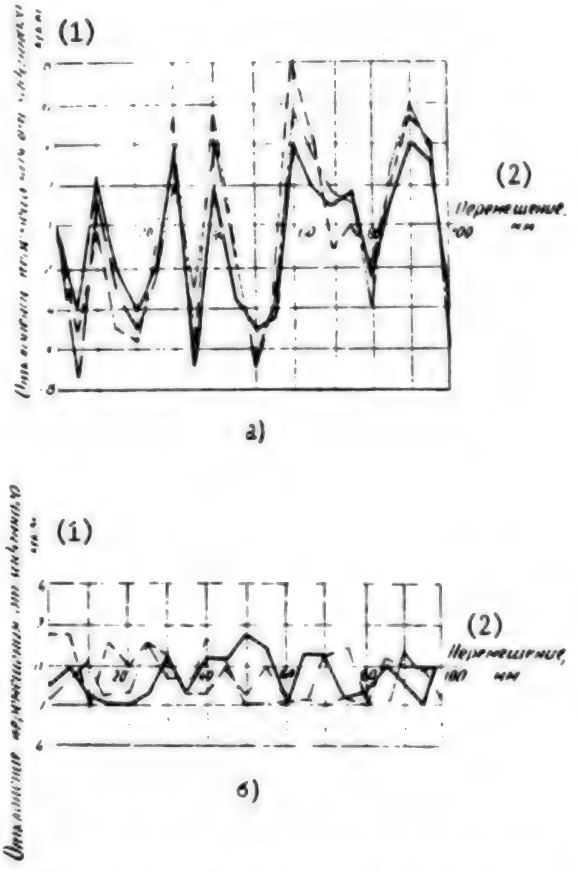

Figure 1. Precision of Positioning the Support of a 16B04P Lathe Equipped With an NC System

Key: a. open-loop control system; b. closed-loop control system with a laser interferometer as the feedback sensor; 1. deviation of movement from the specified; 2. displacement, 100 mm

When a stepping motor is used in closed-loop feed systems of precision lathes, it is necessary to consider that the amount of the stepping motor's discreteness should be an order of magnitude less than the allowable error, which, in view of the limitation of the maximum speed, does not make it possible to obtain sufficiently high idling speeds.

To estimate the precision of positioning the support of a TPK-125VN machine tool with a stepping motor and roller guides, a laser interferometer is mounted directly on the machine tool. A program moves the support 100 mm divided into 10 intervals of 10 mm each. The approach to the bounds of the intervals is bilateral. The positioning precision was estimated in accordance with a method described elsewhere.[1] The systematic error of positioning the support reaches 2 μm, and the random

error amounts to plus or minus 4 μm, with the nonlinearity of the screw-nut kinematic pair making a large contribution (on the order of 3 μm). The appearance of machine tools with aerostatic guides that virtually exclude relaxation vibrations during low feeds and the use of friction mechanical gearings with pretightening in closed-loop feed drives make it possible to obtain small feeds with a high precision and stability at a rather high idling speed.[6] Figure 2 presents a diagram of the feed drive of a TPARM-100 lathe module where aerostatic guides, a direct current motor with a closed friction mechanical gearing providing a movement of 0.6 mm in one rotation of the direct current motor, and a laser interferometer in the feedback circuit of the direct current motor's control system are used.

To analyze the precision characteristics of the feed drive of a TPARM-100 precision lathe module, measurements were made of the repeatability of the support's movement (according to a program) to specified points in the live zone. The deviations of the support's motion from the specified motion in the case of a unilateral approach to the check point, as fixed by a MINICOM (Japan) inductive sensor with a division value of 0.1 μm, are characterized by a mean value not exceeding 0.2 μm.

The combined use of a friction mechanical gearing, a laser interferometer, and aerostatic guides in a TPARM-100 precision lathe module makes it possible to obtain a precision quality of 3 to 4 when finishing (with a cutting force up to 100 N) components with dimensions up to 50 mm. The comparative characteristics of the precision of positioning different feed drives is presented in the table [note: the table is not included in the source text].

Conclusions

1. In view of a number of physical effects, achieving high positioning precision on lathes with sliding guideways is, in principle, complicated—even under conditions where a high-precision feedback sensor, i.e., a laser interferometer, is used.

2. Providing a positioning precision on the order of 1-2 μm in machine tools with sliding guideways entails minimizing the nonlinearities in the screw-nut mechanical transmission of the feed drive.

3. The positioning precision of the support of a TPARM-100 module may be increased to 0.2 μm by using a closed friction mechanical gearing, aerostatic guideways, and a laser interferometer as a feedback sensor in the feed drive, which guarantees machining of components with dimensions up to 50 mm with a quality level of 3 to 4.

Bibliography

1. Pronikov, A. S., ed., "Tochnost i nadezhnost stankov s ChPU" [Precision and Reliability of NC Machine Tools], Moscow, Mashinostroyeniye, 1982, 256 pages.

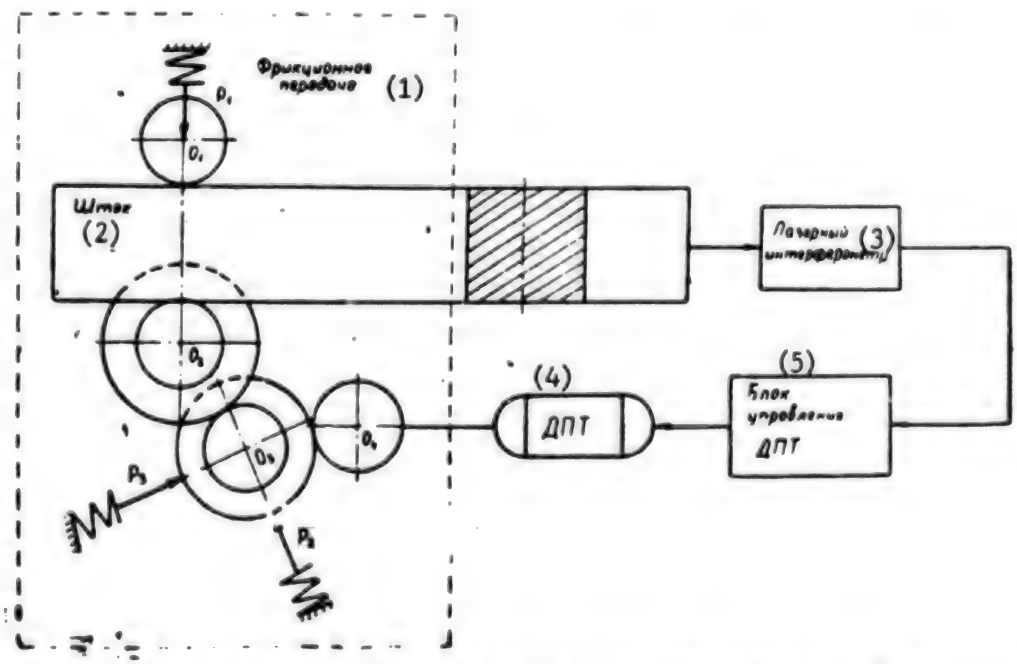

Figure 2. Diagram of the Feed Drive of a TPARM-100 Precision Module, Where P_1, P_2, and P_3 Are Forces Specified by the Device Prior to Tightening of the Friction Rollers O_1 Through O_4

Key: 1. friction gearing; 2. rod; 3. laser interferometer; 4. direct current motor; 5. direct current motor's control unit

2. Ratmirov, V. A., "Upravleniye stankami gibkikh proizvodstvennykh sistem" [Controlling Machine Tools in FMS], Moscow, Mashinostroyeniye, 1987, 272 pages.

3. Pushch, V. E., "Malyye peremeshcheniya v stankakh" [Small Displacements in Machine Tools], Moscow, Mashgiz, 1961, 123 pages.

4. Brzhozovskiy, B. M., Ignatyev, A. A., and Martynov, V. V., "Investigation of Precision Characteristics of Laser Interferometer as Transducer for NC Lathe," IZVESTIYA VYSSHIKH UCHEBNYKH ZAVEDENIY: MASHINOSTROYENIYE, No 9, 1984, pp 149-152.

5. Zatsman, I. R., Bruk, L. I., Zaytsev, S. I., et al., Inventor's certificate 1144774, Lathe, OTKRYTIYA IZOBRETENIYA, No 10, 1985, p 31.

COPYRIGHT: "Izvestiya VUZov. Mashinostroyeniye", 1990.

UDC 658.52.01.56:621.757

Classification of Automatic Assembly Equipment

907F0305G Moscow IZVESTIYA VYSSHIKH UCHEBNYKH ZAVEDENIY: MASHINOSTROYENIYE in Russian No 3, Mar 90 (manuscript received 15 June 88) pp 130-132

[Article by V. A. Serenko, candidate of technical sciences and docent, and V. G. Belomestnov, graduate student; first paragraph is IZVESTIYA VYSSHIKH UCHEBNYKH ZAVEDENIY: MASHINOSTROYENIYE abstract]

[Text] This article presents classifiers of automatic assembly equipment and gripping mechanisms for industrial robots. It is shown that the given classification systems may serve as the basis for developing mathematical models and constructing an equipment data base in a CAD system.

In view of the of the task of designing an assembly manufacturing process, a CAD system must be used. One of the most difficult and hardest-to-formalize tasks, particularly under conditions of flexible manufacturing systems [FMS], is that of selecting automatic assembly equipment. To perform this task, a structuromorphological classification system for automatic assembly equipment was compiled on the basis of an analysis of industrial and literature data.[1-3]

The classification system is a matrix containing a semantic divider in its lines and specific semantic information, i.e., a feature for each of the semantic dividers, in its columns. A set of approaches to constructing structuromorphological classification systems exists.[4,5] We have used the most popular functional approach, i.e., the one based on the principle of the effect and the principal functions performed by equipment. The functions of the equipment under examination or its elements have been selected as semantic dividers (features), and the different methods of implementing each function have been selected as properties (alternative versions). In the classification system equipment is divided into eight groups; however, not all lines are completely filled. This is, first, because only the most important properties of the equipment were considered and, second, because free spots in the classification system may characterize possible prospects for development of the given property of the equipment.

Table 1. Structuromorphological Classification System for Automatic Assembly Equipment

No.	Semantic Divider	Property							
		1	2	3	4	5	6	7	8
1	Type of assembly equipment	Mechanized position	Semiautomatic position	Single-position automaton	Multiposition automaton	Assembly center	Robotic system	Retoolable line	Flexible assembly system
2	Type of production equipment	Welding	Threading	Pressing	Forming	Transport	Gluing	Painting	—
3	Principal configurations	Individual position	Nonordered arrangement	Linear	Circular	—	—	—	—
4	Assembly robots' coordinate systems	Hinged in horizontal plane	Hinged in vertical plane	Rectangular	Cylindrical	—	—	—	—
5	Robots' gripping mechanisms	Based on principle of effect	Based on basing method	Based on type of control	Based on centering method	Based on nature of fastening	—	—	—
6	Storage devices	Vibrating bin	Bin	Readjustable bin	Magazine	Cassette	Coordinate table	—	—

Table 1. Structuromorphological Classification System for Automatic Assembly Equipment (Continued)

No.	Semantic Divider	Property							
7	Orientation devices	Structural asymmetry	Asymmetry of physico-mechanical properties	Cut plates	Automatic search devices	Tactile sensors	Robovision systems	—	—
8	Transport devices	Boats	Cassettes	Conveyers	Conveyers with pallets	Robots	Robocars	—	—

The first line of the table examines the type of assembly equipment. It may be noted that the types of assembly equipment are characterized by flexibility, productivity, and degree of automation. The second line characterizes production equipment, i.e., the equipment that is most frequently used to make joints (connections) directly. It is distinguished mainly by its operating principle. The third line separates the four main configurations of assembly equipment. All of the other configurations are obtained by combinations of these four. The fourth semantic divider examines configurations of industrial assembly robots as the most widely used type of assembly equipment. Equipment hinged in the horizontal plane has enjoyed the most popularity. The fifth line examines the classification of gripping mechanisms as the most important nodes of robots intended for direct manipulation of components. The sixth, seventh, and eighth lines classify devices for storing, orienting, and transporting components.

This classification system makes it possible to collect more complete information about a set of equipment characteristics that are not mutually connected. It should be noted that the classification system may have a hierarchical structure, i.e., a structuromorphological classification system may in turn be compiled on the basis of each line in the table. This is evident from Table 2, which represents a structuromorphological classification system of industrial robot gripping mechanisms. The properties of gripping mechanisms from the columns of Table 1 become semantic dividers, i.e., the lines of Table 2. Breaking down a classification system in this manner makes it possible to consider a large number of features and the nature of their mutual effect in addition to makling it possible to describe a classification system with a treelike structure. When necessary, each element in the table may be given its own "weight," and equipment may be evaluated in accordance with a digital code method.

Table 2. Structuromorphological Classification System for Industrial Robot Gripping Mechanisms

No	Semantic Divider	Property							
		1	2	3	4	5	6	7	8
1	Principle of effect	Clamping	Holding	Attracting	—	—	—	—	—
2	Method of basing	Centering	Basing	Fixing	Manipulating	—	—	—	—
3	Type of control	Uncontrolled	Instructional	Programmable	Adaptive	—	—	—	—
4	Holding method	Mechanical	Electromagnetic	Vacuum	Stream	Chamber	Gravitation	Electrostatic	Adhesion
5	Grip mounting	Unchangeable	Changeable	Quick-change	Revolving adjustment	Automatic magazine	—	—	—

The classification systems presented above make it possible to perform the task of formalizing assembly equipment in a CAD system with an allowance for a large number of characteristics possessing a hierarchical structure (in the form of a tree graph), which significantly simplifies the task of constructing mathematical models and creating data bases, thereby making it possible to identify the most important properties at each level of detailization and to include models of lower-lying levels into higher-lying ones.

Conclusions

1. Structuromorphological classification systems have been proposed for automatic assembly equipment and industrial robot gripping mechanisms.

2. It has been shown that these classification systems may serve as the foundation for constructing mathematical models and creating equipment data bases in CAD systems.

Bibliography

1. Kostyuk, V. I., Yampolskiy, L. S., and Ivanenko, I. B., "Promyshlennyye roboty v sborochnom proizvodstve" [Industrial Robots in Assembly Production], Kiev, Tekhnika, 1983, 183 pages.

2. Kozyrev, Yu. G., "Promyshlennyye roboty: Spravochnik" [Industrial Robots: Manual], 2nd ed., revised and enlarged, Moscow, Mashinostroyeniye, 1988, 392 pages.

3. Korsakov, V. S., and Zamyatin, V. K., ed., "Sborka i montazh izdeliy mashinostroyeniya. T. 1. Sborka izdeliy mashinostroyeniya" [Assembly and Installation of Machine Building Products. Vol 1. Assembly of Machine Building Products], Moscow, Mashinostroyeniye, 1985, 480 pages.

4. Odrin, V. M., and Kartavov, S. S., "Morfologicheskiy analiz sistem" [Morphological Analysis of Systems], Naukova dumka, 1977, 148 pages.

5. Polovinkin, A. I., "Osnovy inzhenernogo tvorchestva: Ucheb. posobiye dlya studentov vtuzov" [Foundations of Engineering Creation. Textbook for Students at Higher Technical Schools], Moscow, Mashinostroyeniye, 1988, 368 pages.

COPYRIGHT: "Izvestiya VUZov. Mashinostroyeniye", 1990.

UDC 621.91.04

Assessing Design Decisions in Manufacturing Process CAD System by Simulation of Process of Manufacturing Components Under FMS Conditions

907F0305F Moscow IZVESTIYA VYSSHIKH UCHEBNYKH ZAVEDENIY: MASHINOSTROYENIYE in Russian No 3, Mar 90 pp 127-130

[Article by V. A. Tsekhmeystruk and M. S. Ukolov, candidates of technical sciences; first two paragraphs are IZVESTIYA VYSSHIKH UCHEBNYKH ZAVEDENIY: MASHINOSTROYENIYE abstract]

[Text] This article examines a simulation and a method of simulating the processes of manufacturing components under the conditions of flexible manufacturing systems [FMS]. The model and method have been developed to analyze alternative versions of a process for manufacturing components in a manufacturing process CAD system that considers the structure of the manufacturing process, the reliability of the tools and equipment used, and different random events occurring when a batch of components is manufactured.

The distinctive features of the construction of the model and simulation method are examined along with selected criteria for evaluating alternative versions of a manufacturing process and the results of verification of the simulation.

The efficient functioning of FMS requires scientific-technical validation and careful assessment of all decisions made as early as in the state when manufacturing processes are designed in a manufacturing process CAD system. It is necessary to consider a whole set of interconnected factors (the parameters of alternative versions of the manufacturing processes; the probabilistic nature of the process of manufacturing components; the reliability of selected tools, attachments, and equipment; etc.). It is advisable to consider the specified factors when evaluating the design decisions used by developing a computer simulation of the processes entailed in manufacturing components under conditions of an FMS.[1-3]

Different methods exist for constructing simulations of the process of the functioning of FMS. Specifically, there are methods that have been developed on the basis of the method of the dynamics of averages, queuing theory, etc.[3-5] These methods make it possible to select the most rational configuration of an FMS, analyze the operation of its transport system, determine the required number of transport carriages or robocars, select their speed, and determine the routes of components' movement between the warehouse and machine tools. The existing methods do not, however, make it possible to compare and select the best versions of processes for manufacturing components among proposed alternative versions since they are based on previously existing manufacturing processes.

To assess the different versions of manufacturing processes in the design stage in a manufacturing process CAD system, a method of simulating the process of manufacturing components in an FMS has been proposed that has a number of fundamental differences from existing methods.

The essence of the method is as follows. In the simulation, the process of manufacturing components is represented by sequentially changing the manufacturing system's states as a function of the structure of the version of the manufacturing process under analysis as well as a function of random events and failures. A specific slice of time is placed in correspondence with one of the manufacturing process's states (for example, the beginning and end of the operation of the i-th tool, j-th machine tool, moments of failures, and restoration of the performability of tools, attachments, or equipment). Each of a manufacturing process's states has a consequence, i.e., it has an effect on the subsequent development of events that is not, for example, considered in queuing systems.

The versions of manufacturing processes developed may have different structures, different tools, different cycle durations, and other differences, which is also considered during the simulation.

When the process of manufacturing components is modeled, time intervals of uninterrupted work are alternated with time intervals in which failed tools and equipment are restored to working order and with time intervals in

which scheduled shutdowns are conducted to maintain and clean machine tools and readjust equipment.

The modeling is performed for each alternative version of the manufacturing process entailed in manufacturing a batch of components. The criteria for evaluating each version are as follows: manufacturing productivity Q_{tex}, technical utilization coefficient η_{tex}, and time required to manufacture a batch of components in accordance with the specified (analyzed) version of the manufacturing process θ_{tex}:

$$Q_{tex} = \frac{\gamma \cdot P}{t_{(1)} + \left(\sum_{i2=0}^{N_2} \tau_{ai_{i2}}^{(3)} + \sum_{i1=0}^{N_3} \tau_{BO_{i3}} + \sum_{i4=0}^{N_4} \tau_{ni_{i4}}^{(4)} + \sum_{i5=0}^{N_5} \tau_{neр_{i5}} \right) / Z_D};$$

$$\Psi_{tex} = \sum_{i1=1}^{N_1} \tau_{0i_{i1}}^{(2)} \sum_{i2=0}^{N_2} \tau_{ai_{i2}}^{(3)} \sum_{i3=0}^{N_3} \tau_{BO_{i3}} \sum_{i4=0}^{N_4} \tau_{ni_{i4}}^{(4)} \sum_{i5=0}^{N_5} \tau_{neр_{i5}};$$

$$\eta_{tex} = \frac{\sum_{i1=1}^{N_1} \tau_{0i_{i1}}^{(2)}}{\Psi_{tex}};$$

where (1) is the duration of the operating cycle; P is the number of components manufactured in one cycle; γ is the coefficient of the output of acceptable product; Z_d is the batch size; (2) represents the intervals of uninterrupted operation; (3), τ_{BO}, (4), and $\tau_{пер}$ are the durations of interruptions owing to failures of tools, failures of equipment, the taking of scheduled measures, and readjustments; and N_1, N_2, N_3, N_4, and N_5 are the number of different types of time intervals derived during modeling.

Time losses due to technical organization factors are not considered since they depend on the nature and operation of the FMS rather than on the parameters of the manufacturing process.

During computer simulation, the version of the manufacturing process being analyzed is repeated many times (50 realizations), with different combinations of all-possible random events occurring during the process of manufacturing the components being derived. The results of each realization are stored and subjected to statistical processing in the culminating stage. The average values and maximum and minimum values of the technical productivity, coefficient of technical utilization, durations of the interruptions due to various causes, average number of failures per period of machining a batch of components, etc., are printed out.

A simulation of the process of manufacturing components in an FMS was realized in the form of a program for a model YeS-1022 computer. The program is written in the language FORTRAN-4.

The sensitivity of the simulation developed to the variations in the initial parameters was assessed. When the experiment evaluating the simulation's sensitivity was planned, the model's parameters were varied on two levels within the bounds of scattering plus or minus 5 percent of the mean level. The number of experiments was reduced by using a type 2^{5-2} fractional factor experiment.[6]

The results of the assessment of the sensitivity of the simulation developed showed its adequate stability in the face of variations in the parameters. Thus, with a scattering of the values of the model's initial parameters equal to plus or minus 5 percent, the resultant technical productivity values had a scattering of the mean values of plus or minus 1.28 percent, with maximum bounds of plus or minus 1.42 percent and minimum bounds of plus or minus 3.68 percent.

Using the simulation method and computer program developed as a subsystem to analyze alternative versions of a manufacturing process makes it possible to select the best version not only from the standpoint of mean efficiency criterion indicators but also from the standpoint of the stability of their preservation in the process of machining a batch of components. This is particularly important for conditions of technologies using few workers.

Bibliography

1. Azbel, V. O., Yegorov, V. A., and Zvonitskiy, A. Yu., "Gibkoye avtomaticheskoye proizvodstvo" [Computer-Integrated Manufacturing], ed. by S. A. Mayorov and G. V. Orlovskiy, 2nd ed., revised and enlarged, Kh., Mashinostroyeniye, 1985, 454 pages.

2. Henly, E. D., and Kumamoto, X., "Reliability of Engineering Systems and Risk Assessment," translated from English by V. S. Syromyatnikov and G. S. Demina, ed. by V. S. Syromyatnikov, Moscow, Mashinostroyeniye, 1984, 528 pages.

3. Portman, V. G., Barabanov, V. V., Kardanskiy, L. A., et al., "Nadezhnost i effektivnost ispolzovaniya oborudovaniya avtomatizirovannykh kompleksov" [Reliability and Effectiveness of Using Equipment of Automated Systems], Obzor NIImash [Review of Machine Building and Machining SRI], 1975, 75 pages.

4. Dashchenko, A. I., "Statistical Modeling of Manufacturing Machine Systems, in "Nauchnyye osnovy progressivnoy tekhniki i tekhnologii" [Scientific Principles of Progressive Engineering and Technology], Moscow, Mashinostroyeniye, 1985, pp 276-305.

5. Spur, G., Hirn, W., Seliger, G., and Viehweger, B., "Simulation zur Auslegungs und Optimiezung von Productions systemen," ZEITSCHRIFT FUR WIRTECHNAFTLICHE FERTIGUNG, B 77, No 9, 1982, pp 446-452.

6. Adler, Yu. P., et al., "Planirovaniye eksperimenta pri poiske optimalnykh usloviy" [Planning Experiment When Searching For Optimum Conditions], Moscow, Nauka, 1971, 283 pages.

COPYRIGHT: "Izvestiya VUZov. Mashinostroyeniye", 1990.

UDC 621.822.9

Conducting Service Life Tests on Flexible Bearings for Strain-Wave Gearing on Special Stands

907F0305A Moscow IZVESTIYA VYSSHIKH UCHEBNYKH ZAVEDENIY: MASHINOSTROYENIYE in Russian No 3, Mar 90 (manuscript received 18 Jul 89) pp 25-27

[Article by V. A. Finogenov, candidate of technical sciences and docent, and Ye. A. Sarayev, graduate student; first paragraph is IZVESTIYA VYSSHIKH UCHEBNYKH ZAVEDENIY: MASHINOSTROYENIYE abstract]

[Text] A design for a special stand for conducting tests on flexible bearings of strain-wave gearings is proposed. The stand's design makes it possible to simulate the conditions of the loading of flexible bearings in an actual strain-wave gearing.

It is known that achieving more reliability and better predictability of test results is possible with experimental research of the performability of large groups of components or machinery subassemblies under identical loading conditions. The specified conditions must also be observed when forecasting the durability of flexible bearings for strain-wave gearings.

From the standpoint of design dimensions, flexible bearings are close to radial rolling ball bearings in the ultralight series; however, they have thinner rings and a retainer with a crown design and increased gaps between its connectors and balls. In the the strain-wave gearing the flexible bearing is mounted on an oval cam, during the rotation of which the outer ring undergoes a cyclically changing buckling stress. The flexible bearing's balls move with a variable speed, which changes the gap between the retainer's connectors and the balls from zero to the maximum. A portion of the balls drive the retainer, and another portion brakes it. This interaction of the rollers and retainer causes an increased (compared with that in conventional roller bearings) slide of the balls along the raceways and strong contact of the latter with the retainer's connectors.

The distinction of the design application of flexible bearings is as follows: the oval form of the rings, along with the specifics of its loading in a strain-wave gearing (i.e., the fact that it receives an unevenly distributed load from the engagement in several zones, the amount of which depends on the number of the flexible gear's deformation waves), excludes the possibility of using the existing stands[1] that the bearing industry uses to test ball bearings when testing flexible bearings.

The distribution of the load in each of the zones of a flexible bearing is determined by many factors: the amount of deformation of the flexible gear, the stiffness and precision with which it has been manufactured or assembled, and also the degree of wear to the main elements of the strain-wave gearing.

In view of the fact that standard flexible bearings for strain-wave gearings are currently being series-produced by the bearing industry, the task of forecasting their service life under different conditions of strain-wave gearings' operation and their structural variety is critical. For these purposes, the All-Union Scientific Research Institute of the Bearing Industry and the Moscow Higher Technical School imeni N. E. Bauman developed stands for conducting experimental research on flexible bearings for strain-wave gearings that made it possible to conduct comparative tests to determine their optimum design parameters during the period of the development of the All-Union State Standard[2] for these bearings. However, the loading conditions of flexible bearings on these stands did not conform to their loading conditions in an actual strain-wave gearing.

The correctness of service life tests of flexible bearings for the purpose of determining their dynamic payload capacity is largely dependent on the stability of the testing mode, which may be ensured only in the case where the tests are conducted on special stands equipped with monitoring and recording equipment. In view of this, determining the actual service life of standard flexible bearings requires developing a type-and-size series of special test stands that make the conditions of testing flexible bearings as close as possible to the conditions of their operation in strain-wave gearings. In our opinion, the SiGP MGTU stand for testing No 824 standard flexible bearings that was developed and manufactured at the Moscow Higher Technical School imeni N. E. Bauman in the machinery components department* may serve as the basis for developing such a series.

Figure 1 presents a design diagram of the stand. The stand consists of a loading mechanism (1) whose shaft is set into rotation by an electric motor (2) through a flexible coupling (3), a counter (4) that counts the number of rotations, and monitoring and recording equipment (not shown in Figure 1).

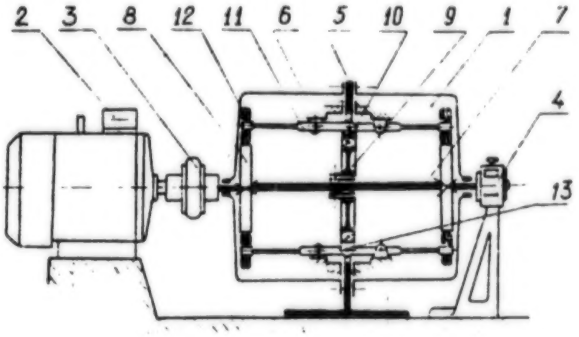

Figure 1

The loading mechanism is implemented in a separate case consisting of a pedestal (5) and caps (6), it has a symmetrical design, and it consists of the following main assemblies: a shaft (7) with loading cams (8), an oval cam (9) (with a flexible bearing (10), i.e., the object under investigation) that is hinged to a shaft (7) and equidistant from the loading cams (8) and levers (11), which are evenly distributed in a circular direction and hinged to the pedestal (5). With one arm, the levers (11) make contact with the loading cams (8) through the rollers (12), and with the other arm they make contact with the outer ring of the flexible bearing (10) through shoes (13).

In the event of elastic deformation of the levers (11), the loading cams (8) create a discrete load on the flexible bearing (10). To reduce the discreteness of the load's application, the stand is provided with the maximum possible number of levers (11) (24 flexible bearings), with each shoe (13) interacting with the outer ring of the flexible bearing (10) along two narrow contact sites. The loading law governing the flexible bearing is specified by the profile of the replaceable loading cams, with the load on the flexible bearing turning with a frequency equal to the rotation frequency of the oval cam (shaft 7).

Technical Characteristics of the Stand

Flexible bearing undergoing testing	No 824
Rotation frequency of flexible bearing's inner ring	0 to 1,500 min^{-1}
Maximum radial load on flexible bearing	3,000 N
Usable lubricants	plastic, liquid

Devices for selecting the play and compensating for the wear of the friction pair have been provided in the stand's design.

The monitoring and recording equipment of the SiGP MGTU stand provide for the following:

—readout of the loading cycles, monitoring of the magnitude of the load on the flexible bearing and the stability of the rotation frequency of its inner ring, heat stabilization of the oil in the zone of the flexible bearing, ad the capability of emergency automatic shutoff of the electric motor in cases where the object being investigated malfunctions or fails during operation of the stand's loading elements.

Parallel preliminary tests of a No 824 flexible bearing on an SiGP MGTU stand and in a real strain-wave gearing showed the identity of the qualitative changes in the components of both flexible bearings tested, which confirms the possibility of using the stand for service life tests of flexible bearings.

Bibliography

1. Reshetov, D. N., ed., "Mashiny i stendy dlya ispytaniya detaley" [Machines and Stands for Testing Components], Moscow, Mashinostroyeniye, 1979, pp 265-303.

2. "Podshipniki gibkiye sharikovyye radialnyye. Osnovyye razmery" [Flexible Radial Ball Bearings. Main Sizes], GOST 23179-78.

Footnote

*There is an All-Union Scientific Research Institute of the State Patent Commission of Experts [VNIIGPE] decision regarding acknowledging the proposed stand as an invention and issuing a patent certificate.

COPYRIGHT: "Izvestiya VUZov. Mashinostroyeniye", 1990.

END OF FICHE

DATE FILMED

15 Aug. 1990